Supplementary Information for:

Escape Tectonics: Early Miocene Synchronous Onset of the North and East Anatolian Transform Faults

Volkan Karabacak, I. Tonguç Uysal, Aynur Dikbaş, Feng Liang, Manuel Curzi, Eugenio Carminati, Mesut Aygül, İsmet Elma, Jian-xin Zhao

Summary

This Supplementary Information file provides background information on the geodynamic setting, fault rocks, additional field structural and kinematic data, geochronological data in support of the main manuscript and references. The dataset documents early Miocene to late Pleistocene syntectonic carbonate growth within the East Anatolian Fault (EAF) corridor.

Geological setting

The tectonic evolution of the Eastern Mediterranean region is fundamentally governed by the northward movement of the Arabian Plate. This plate began behaving as a distinct tectonic entity during the early Miocene, a process that coincided with the opening of the Red Sea (Quennell, 1958; McKenzie, 1970; Garfunkel, 1981; Hempton, 1987; Steinz, Bartov, 1991; Garfunkel, Ben-Avraham, 1996). Once separated, the Arabian Plate advanced toward and collided with the Eurasian Plate at a convergence rate of roughly 18–25 mm per year (Jolivet & Faccenna, 2000). The progressive Arabia–Eurasia convergence transitioned from ‘soft collision’ (subduction of the hyperextended continental margin) to ‘hard collision’ (continental underthrusting) at ~20 Ma with the onset of regional exhumation along the BZSZ, driving major tectonic reorganization along the zone (Darin & Umhoefer, 2022; Okay et al., 2010).

At the same time, lithospheric extension was taking place farther west in the Aegean region. This extension was associated with slab rollback processes along the Hellenic and Cyprus subduction zones, which began during the same period (Seyitoğlu et al., 1992; Ring et al., 2010). The synchronous occurrence of compressional tectonics in the east and extensional tectonics in the west underscores the interconnected nature of tectonic processes throughout the broader Eastern Mediterranean domain (Le Pichon & Kreemer, 2010).

The convergence and ensuing tectonic reorganization not only resulted in the uplift of Eastern Anatolia but also established the structural framework necessary for major strike-slip fault systems to develop. Among these, the NAF and the EAF emerged as significant features, playing critical roles in facilitating the westward "escape" or

extrusion of the Anatolian Block. This lateral displacement is closely linked to earlier vertical tectonic processes, specifically uplift driven by crustal thickening, shortening, and asthenospheric upwelling. These processes increased the potential energy within the plateau (Şengör et al., 2005; Le Pichon & Kreemer, 2010; Ring et al., 2010; van Hinsbergen et al., 2024). The resulting gravitational potential gradient between the high Eastern Anatolian Plateau and the extensional Aegean domain is thought to have been a major force driving Anatolia's westward motion.

Geochronological and geochemical syntheses for the Caucasus–Iran–Anatolia (CIA) volcanic province further indicate that post-collisional magmatism initiated diachronously and evolved through distinct stages. Lin et al. (2020) document an onset at ~17 Ma in SE Anatolia, followed by a northward propagation toward NE Anatolia and NW Iran during ~11–9 Ma, and interpret this pattern in terms of a two-stage (double) slab-breakoff process. They further suggest that after ~6.5 Ma volcanism became widespread and compositionally heterogeneous due to wholesale lithospheric delamination, and that from ~2 Ma activity waned in western Eastern Anatolia while migrating eastward–southeastward toward Iran, consistent with oblique collision and continental extrusion.

Located between the Pontide arc to the north and the converging Arabian Plate to the south, East Anatolia forms a high-elevation (>1.5–2.0 km), dome-shaped, actively deforming plateau, with its elevation supported by upwelling hot mantle (Keskin, 2003; Göğüş & Pysklywec, 2008) (Fig. 1A). Following the diachronous (late Eocene to middle Miocene) Arabia-Eurasia collision (Darin and Umhoefer, 2022), the region experienced N-S shortening and the development of predominantly strike-slip faulting (Şengör et al 1985), accompanied by diachronous post-collisional magmatism that initiated as early as ~17 Ma in SE Anatolia and migrated across the CIA region through the Late Miocene (Keskin, 2003; Lin et al., 2020). This diachroneity complicates attempts to link any single deformation phase to the onset of a particular strike-slip fault system. Nevertheless, geodetic and geological datasets converge on the view that the present plate boundary between Anatolia and Arabia is dominantly strike-slip (Reilinger et al., 2006). A summary of differing interpretations regarding the timing and nature of the tectonic mechanisms that shaped the geodynamic evolution of the Eastern Mediterranean is provided in the accompanying table (Supplementary Information, Table S1).

The EAF forms a ~600 km-long, NE–SW-trending sinistral strike-slip system linking the Karlıova triple junction (NAF–EAF–Varto/Ovacık systems) to the south-west where deformation is transferred to the DST and the Cyprus–Levant margin. It is composed of a series of parallel and sub-parallel left-lateral strike-slip faults with locally significant normal components and consists of fault segments separated by jog structures such as fault stepovers and bends (e.g., Şaroğlu et al., 1992; Karabacak et al., 2012; Duman, Emre, 2013; Curzi et al., 2026) (Fig. 1B); this segmentation strongly influences rupture extent and local slip partitioning.

Published GPS slip rates for EAF range from ~4–13 mm/year depending on the segment and methodology (Reilinger et al., 2006; Aktuğ et al., 2016), while geodetic and geomorphological estimates range from as low as ~1–5 mm/year in some models to as high as ~8–9 mm/year in others (Duman & Emre, 2013; Yönlü et al., 2017; Karabacak et al., 2023; Yönlü & Karabacak, 2024; Dikbaş & Önal, 2025). These values, summarised in Supplementary Information Table S2, highlight strong segmentation and structural complexity along the direction (Emre et al., 2018) and help explaining why some segments appear partially creeping, weakly

interlocked or fully locked. Recent observations also indicate heterogeneous near-surface locking and local creep/afterslip; for example, shallow creep along the Palu Segment has been proposed in the context of rupture arrest during the 2020 Mw 6.8 Elazığ earthquake along the Pütürge Segment (Çakir et al., 2023). The 2023 Kahramanmaraş earthquake sequence also manifest the aspects of fault "maturity" that may facilitate fracture transfer and multi-segment linkage (Karabacak et al., 2023; Provost et al., 2024).

A synthesis of long-term cumulative left-lateral displacements along the EAF (Supplementary Information Table S3) reveals that displacements generally cluster between 9 and 27 km, with consistent estimates of ~22 km in the northeast and ~16 km in the southwest (Gölbaşı region). These estimates are based on displaced volcanic units, stratigraphic contacts, and river valleys (Arpat & Şaroğlu, 1972; Hempton, 1985; Herece & Akay, 1992; Karabacak et al., 2012 and related references).

Supplementary Table S1. Evolutionary timeline of the Eastern Mediterranean and associated geological evidence.

Time interval	Dead Sea Transform	Eastern Anatolian Plateau		East Anatolian Fault	North Anatolian Fault	Aegean Sea (extension/basin development)
		Lithospheric model	Surface geological evidence			
Early Miocene	Left-lateral motion along the Dead Sea Transform (DST) is generally inferred to have initiated in the middle Miocene (Garfunkel, 1981) or the early Miocene (Hempton, 1987; Steinz and Bartov, 1991; Garfunkel and Ben-Avraham, 1996). Onset timing spans 20–17 Ma (Nuriel et al., 2017). Paleomagnetic vertical-axis rotation data from Mesozoic–Cenozoic units along the Bitlis–Zagros suture zone in SE Anatolia (within the Dead Sea Fault–bounded domain) document substantial clockwise block rotations relative to Africa, consistent with pre–middle Miocene DSFZ-related deformation (Bakkal et al., 2019).	Continental collision begins at ~26 Ma; the northern (Pontide) slab starts to peel back under asthenospheric forcing (Çetiner et al., 2025).	Apatite fission-track (AFT) data suggest hard collision onset in the Early Miocene (~20 Ma) along the Bitlis belt (Okay et al., 2010). Diachronous initiation of post-collisional Caucasus–Iran–Anatolia (CIA) volcanism at ~17 Ma in SE Anatolia (Tauride block–Arabian foreland), including early bimodal magmatism indicative of transient extension; volcanism was interpreted as the first stage of a double slab breakoff (Lin et al., 2020).	Original dates of syn-kinematic mineralizations indicate an Early Miocene onset for fault localization (~22 Ma) **(this study)**	Late Oligocene–Early Miocene (~25–20 Ma) fault gouge ages from dextral fault structures in the eastern NAF (Uysal et al., 2006; Boles et al., 2015; Uysal et al., 2025).	Onset of Aegean lithospheric-scale extension in the Late Oligocene–Early Miocene (~23 Ma) (Seyitoğlu et al., 1992; Ring et al., 2010).
Late Miocene	—	~10 Ma: break-off of the northern slab; opening of an asthenospheric window; onset of rapid uplift in the north of Anatolia; southward propagation of asthenosphere; steepening of the southern slab (Çetiner et al., 2025).	The southward-younging volcanism pattern proposed by Keskin (2003) (e.g., Nemrut, Süphan, Tendürek in the southern half of the plateau) is interpreted as the surface expression of this late tectonic phase (break-off/delamination). Across the broader CIA province, volcanism migrates in space and time, reaching NE Anatolia–NW Iran by ~11–9 Ma, which Lin et al. (2020) relate to a second slab-breakoff episode. Together with slab breakoff/delamination scenarios (e.g., Keskin, 2003), this supports Late Miocene mantle-window/thermal reorganization.	Original dates of syn-kinematic mineralizations indicate further late Miocene localization (~6 Ma) **(this study)** Indirect markers such as volcanic offsets, thermal events, and regional deformation patterns place EAF's onset in the Late Miocene to Pliocene (Arpat & Şaroğlu, 1972; Şengör et al., 1985; Dewey et al., 1986; Hempton, 1987; Lyberis et al., 1992). Collision-scale kinematic budgeting suggests a late Cenozoic reorganization (~5 ± 2 Ma) during which the modern partitioning into major strike-slip systems became established; extrapolated present-day rates over ~3–7 My reproduce finite offsets (Allen et al., 2004). Thermochronology and seismic imaging suggesting the EAF localised as a lithosphere-scale boundary only ~5 Ma ago, in response to strong Arabian underthrusting (Whitney et al., 2023).	Reactivation of the NAF (~11–8 Ma) (Uysal et al., 2006; Boles et al., 2015; Uysal et al., 2025).	—
Plio–Quaternary	—	~2 Ma: southern slab break-off/necking and deformation within the suture belt (Çetiner et al., 2025).	From ~6.5 Ma onward, CIA volcanism became more widespread and compositionally heterogeneous, attributed to wholesale lithospheric delamination (Lin et al., 2020). From ~2 Ma, volcanism waned in the western CIA province and propagated eastward and southeastward toward SE Iran along the Urumieh–Dokhtar magmatic belt, consistent with oblique Arabia–Eurasia collision and continental extrusion (Lin et al., 2020).		Late Cenozoic reorganization and establishment of the modern Anatolian transform framework (Allen et al., 2004).	—

Supplementary Table S2. Slip-rate compilation for EAF segments.

Fault/segment	Slip rate (mm/yr)	Method	Notes	Reference(s)
EAF overall	25-31	Seismological	Variable along-strike; faster in the NE	Taymaz et al., 1991
	6			Kiratzi, 1993
	10±5	GPS		Oral et al., 1992
	15±3			Reilinger et al., 1997
	11±1			Barka and Reilinger, 1997
	9 ±1			McClusky and diğ., 2000
	4.0-4.6			Westaway, 2003
	10±1			Reilinger et al., 2006
	9.7±0.9			Bertrand, 2006
	10.3			Aktuğ et al. 2016
	19	Kinematics		Lyberis et al., 1992
	6			Kiratzi, 1993
	7.8-9			Yürür and Chorowicz, 1998
	6	Geological		Arpat and Şaroğlu, 1972; Seymen and Aydın, 1972; Kiratzi, 1993
	9			Kasapoğlu, 1987; Yürür and Chorowicz, 1998
Karlıova-Ilıca Segments	~8.3	Geological	Northernmost EAF near triple junction	Herece, 2003
	7	Geological	Ilıca segment	Dikbaş & Önal (2025)
Palu Segment	~8.2	Geomorphology / paleoseismic / geodetic	Lake-basin pull-apart influence	Hubert-Ferrari et al., 2020
	8.2±0.2	Geological		Herece, 2003
Pütürge Segment	5	Various (geomorphology, sedimentary basins)	Strongly variable across studies	Koçyigit et al,, 2001
	11			Çetin et al, 2003
	13.5			Güneyli, 2002
	4			Aksoy et al,, 2007
Pazarcık Segment	5.6	Geomorphology & geodesy; Quaternary/ paleoseismic	Segment ruptured in 2023; Quaternary rate ~5.6	Yönlü & Karabacak, 2024
	5.3			Koçyigit et al,, 2001
	1.18			Çetin et al, 2003
	8.85			Güneyli, 2002
	5.6			Aksoy et al,, 2007
Karasu Fault	4.1	Geological/paleoseismic/geodetic	Segment ruptured in 2023; Distributed deformation	Rojay, et al., 2001
	1.0 – 1.6			Yurtmen, et al. 2000
	2.5 ± 1			Bertrand, 2006
	4			Karabacak 2007
	4-4.5			Mahmoud et al. 2013
Dead Sea Fault (northernmost section)	1.9	Geologic/ paleoseismic /geomorphological	Comparable with slip rates along plate boundary	Westaway, 2004
	4.3			Aktuğ et al. 2016
	4.9			Karabacak et al. 2010
	6			Altunel et al 2009

Supplementary Table S3. Displacement constraints used in slip-rate estimates

Fault Segment	Displacement (km)	Marker / Reference Feature	Reference(s)
Ilıca	~22	Volcanic units	Arpat and Şaroğlu (1972); Dewey et al. (1986)
	17	Metamorphic contact	Duman & Emre (2013)
	15	Metamorphic contact	Seymen & Aydın (1972); Dikbaş & Önal (2025)
Palu	27	Mesozoic mudstones	Arpat and Şaroğlu (1972)
	22	Eocene Maden Complex	Koçyiğit et al. (2001)
	9	Eocene Simaki Fm.	Herece and Akay (1992)
Pütürge	15–22	Euphrates River / Bitlis Suture	Arpat and Şaroğlu (1975); Hempton (1985)
	9–13	Geological contacts	Aksoy et al. (2007); Şaroğlu et al. (1987)
Pazarcık	16.5 ± 0.5	Aksu River valley / Gölbaşı basin	Karabacak et al. (2012)
	~16–30	Cretaceous limestones	Westaway and Arger (1996)

Supplementary Table S4. Sample locations and interpreted ages. Note that, some localities yield multiple ages spanning different time domains (e.g., Çobantaş, Harmanlı), interpreted as episodic reactivation.

Segment	Sample		Lon	Lat	Easting	Northing	Site/description	Structure & host	Kinematics (field)	Method	Age (2σ)
Ilıca	ÇOB-2	ÇOB-2-1	40.819315	39.069735	657383	4326081	Limestone quarry east of Çobantaş village Slickenline	Slickenfibre on slip surface; limestone/marble	Sinistral, oblique/transtensional	U–Pb	7.7 ± 2.4 Ma
		ÇOB-2-2	40.819315	39.069735	657383	4326081	Limestone quarry east of Çobantaş village Slickenline	Slickenfibre on slip surface; limestone/marble	Sinistral, oblique/transtensional	U–Pb	6.72 ± 0.62 Ma
	ÇOB-4a		40.819315	39.069735	657382	4326063	Limestone quarry east of Çobantaş village Vein	Composite vein margin (wall-rock contact)	Associated with sinistral shear zone	U–Pb	21.5 ± 4.2 Ma
	ÇOB-4b	ÇOB-4b-1	40.819315	39.069735	657382	4326063	Limestone quarry east of Çobantaş village Vein	Composite vein core (younger fill)	Associated with sinistral shear zone	U–Pb	8.0 ± 1.8 Ma
		ÇOB-4b-2	40.819315	39.069735	657382	4326063	Limestone quarry east of Çobantaş village Vein	Composite vein core (younger fill)	Associated with sinistral shear zone	U–Pb	6.5 ± 1.1 Ma
	HC-C-1		40.821920	39.094588	657305	4328620	South of Hacılar village Vein	N–S vein; damage zone	Near EAF damage structures	U–Th	≥500 ka (secular equilibrium)
Palu	Palu-2		39.950187	38.699686	582676	4283602	Soutwest of Palu village Slickenline	Stepped slickenfibre; limestone interface	Sinistral transtensional	U–Pb	22.60 ± 0.38 Ma
	Palu-3b		39.950187	38.699686	582676	4283602	Soutwest of Palu village Slickenline	Stepped slickenfibre; slip surface	Sinistral transtensional	U–Pb	20.60 ± 0.38 Ma
	Palu-4		39.950187	38.699686	582676	4283602	Soutwest of Palu village Slickenline	Stepped slickenfibre; slip surface	Sinistral transtensional	U–Pb	21.10 ± 0.30 Ma
Pütürge	CGN-2		38.743496	38.172284	477532	4224961	Çaygören Breccia cement	Vein/breccia cement in marble	Damage zone dilation	U–Th	113.8 ± 3.5 ka
	CGN-3		38.743496	38.172284	477532	4224961	Çaygören Breccia cement	Vein/breccia cement in marble	Damage zone dilation	U–Th	44.9 ± 12.8 ka
	TPH-1		38.743534	38.166335	477533	4224301	Tepehan Slickenline	Stepped slickenfibre	Sinistral transtensional	U–Th	≥500 ka (secular equilibrium)
Erkenek	HRM-1		37.840200°	37.745131°	389585	4188827	Harmanlı Village just on the 2023 surface rupture	Calcite vein	Associated with sinistral shear zone	U–Pb	2.6 ± 2.4 Ma
	HRM2		37.840200°	37.745131°	389585	4188827	Harmanlı Village just on the 2023 surface rupture	Calcite vein	Associated with sinistral shear zone	U–Pb	7.28 ± 0.76 Ma
	HRM3		37.840200°	37.745131°	389585	4188827	Harmanlı Village just on the 2023 surface rupture	Stepped slickenfibre	Sinistral	U–Pb	4.0 ± 2.3 Ma
	HRM4		37.840200°	37.745131°	389585	4188827	Harmanlı Village just on the 2023 surface rupture	Calcite vein	Associated with sinistral shear zone	U–Pb	5.55 ± 0.35 Ma
Pazarcık	TRK-1a		37.379450	36.834344	308258	4139168	Türkoğlu Villag	Stepped slickenfibre	Sinistral		21.9 ± 5.8 Ma
	TRK-8		37.379450	36.834344	308258	4139168	Türkoğlu Villag	Vein/breccia cement in marble	Associated with sinistral shear zone	U–Pb	23.63 ± 0.97 Ma

Supplementary Table S5. Structural data.

Location	Coordinates (WGS84-UTM Zone 37/Geographic)	Fault Plane (Strike/Dip)	Rake	Sample
HACILAR (HC)	657305 E / 4328620 N (Z37) 39.092533°/ 40.818936°	N05°W / 85°SW N10°W / 88°SW N05°W / 84°SW N11°W / 80°SW N03°W / 80°SW N10°W / 81°SW N13°W / 85°SW	25°N 18°N 09°N 26°N 34°N 26°N 16°N	
		Veins		
		0°N / 70°W N-S / n.a. N85°E / 90°		
ÇOBANTAŞ (COB)	657383 E / 4326081 N (Z37) 39.069651° / 40.819250°	N40°E / 88°NW N48°E / 85°NW N38°E / 90° N43°E / 87°NW N41°E / 87°NW N36°E / 90° N35°E / 87°NW	25°N 26°N 22°N 29°N 17°N 20°N 22°N	
		Veins		
		N60°E / 88°SE N68°E / 80°SE N68°E / 80°SE 0°N / 64°W 0°N / 85°W		
PALU (PALU)	582676 E / 4283602 N (Z37) 38.697179°/ 39.950730°	N32°E / 85°NW N55°E / 85°NW N55°E / 85°NW N55°E / 82°SE N59°E / 79°SE N24°E / 80°NW N58°E / 81°NW	12°NE 56° 29°NE 43°NE 49°NE 08°NE 22°NE	
ÇAYGÖREN (CGN)	477532 E / 4224961 N (Z37) 38.172278°/ 38.743491°	N72°E / 55°SE N50°E / 50°SE N74°E / 53°SE N67°E / 60°SE N70°E / 60°SE N55°E / 54°SE N74°E / 45°SE	n.a. 65°SE 42°E 57°E 50°E 68°SE 77°SE	
		Veins		
		N20°E / 70°NW		
		Breccia cements		
		N05°E / 78°SE N20°E / 51°SE		
TEPEHAN (TPH)	477364 E / 4224265 N (Z37) 38.166001°/ 38.741596°	N25°E / 58°NW N60°E / 65°NW N68°E / 56°NW N50°E / 75°NW N71°E / 53°NW N66°E / 62°NW N44°E / 81°NW	n.a. 0° n.a. 26°SW 07°NE 05°SW 22°NE	
HARMANLI (HRM)	389585 E / 4188827 N (Z37) 37.840200°/ 37.745131°	N84°E / 76°NW N82°E / 78°NW N80°E / 74°NW N82°E / 59°NW N79°E / 61°NW N65°E / 88°NW N63°E / 87°NW N65°E / 89°NW N67°E / 70°NW N65°E / 71°NW N43°E / 90°NW	0° NW 03° NW 04° NW 16°NW 14°NW 45°NW oblique 47°NW oblique 48°NW oblique 62°NW oblique 63°NW oblique 45°NE	HRM-3
		Calcite veins		

		N15°E / 90° N30°E / 90° N10°E / 90° N05°W / n.a. N10°W / n.a. N30°W / n.a. N30°E / 90° N08°E / 90° N05°E / 90°		HRM-1 HRM-2 HRM-4
OZAN **(OZN)**	384194 E / 4185491 N (Z37) 37.809472°/ 37.684411°	N32°E / 90° N35°E / 90° N34°E / 89° N33°E / 90° N20°W / 60°NE N21°W / 58°NE N18°W / 63°NE N19°W / 61°NE N22°W / 59°NE NW / 75°E	24°SW 22°SW 23°SW 21°SW 32°SE 33°SE 29°SE 30°SE 28°SE 45°S	
TEVEKKELİ **(TVK)**	321903 E / 4146935 N (Z37) 37.452139°/ 36.986494°	N10°E / 55°NW N12°E / 54°NW N12°E / 57°NW N11°E / 56°NW N12°E / 55°NW N14°E / 58°NW N13°E / 57°NW	05°N 07°N 04°N 06°N 05°N 08°N 07°N	
TÜRKOĞLU **(TRK)**	308258 E / 4139168 N (Z37) 37.379450°/ 36.834344°	N68°E / 34°NW N69°E / 36°NW N55°E / 56°NW N55°E / 59°NW N65°E / 52°NW N66°E / 42°NW N60°E / 50°NW N60°E / 50°NW N65°E / 44°NW N66°E / 41°NW N67°E / 43°NW N63°E / 40°NW	10°NE 08°NE 04°NE 06°NE 04°NE 08°NE 0°NE 03°NE 07°NE 12°NE 10°NE 10°NE	TRK-1a / TRK-1b TRK-6 TRK-3 TRK-8
BURKAÇLI **(BRK)**	274153 E / 4119499 N (Z37) 37.194652°/ 36.455425°	N45°E / 65°SE N53°E / 64°SE N42°E / 70°SE N44°E / 71°SE N40°E / 60°SE N41°E / 63°SE N60°E / 80°SE N65°E / 73°SE N63°E / 74°SE N55°E / 60°SE N54°E / 63°SE N52°E / 61°SE	10°NE 60°SE 05°NE 07°NE 80°SE 78°SE 40°SW 76°SW 75°SW 35°SW 36°SW 39°SW	 BRK-5 BRK-4 BRK-1 BRK-3 BRK-2

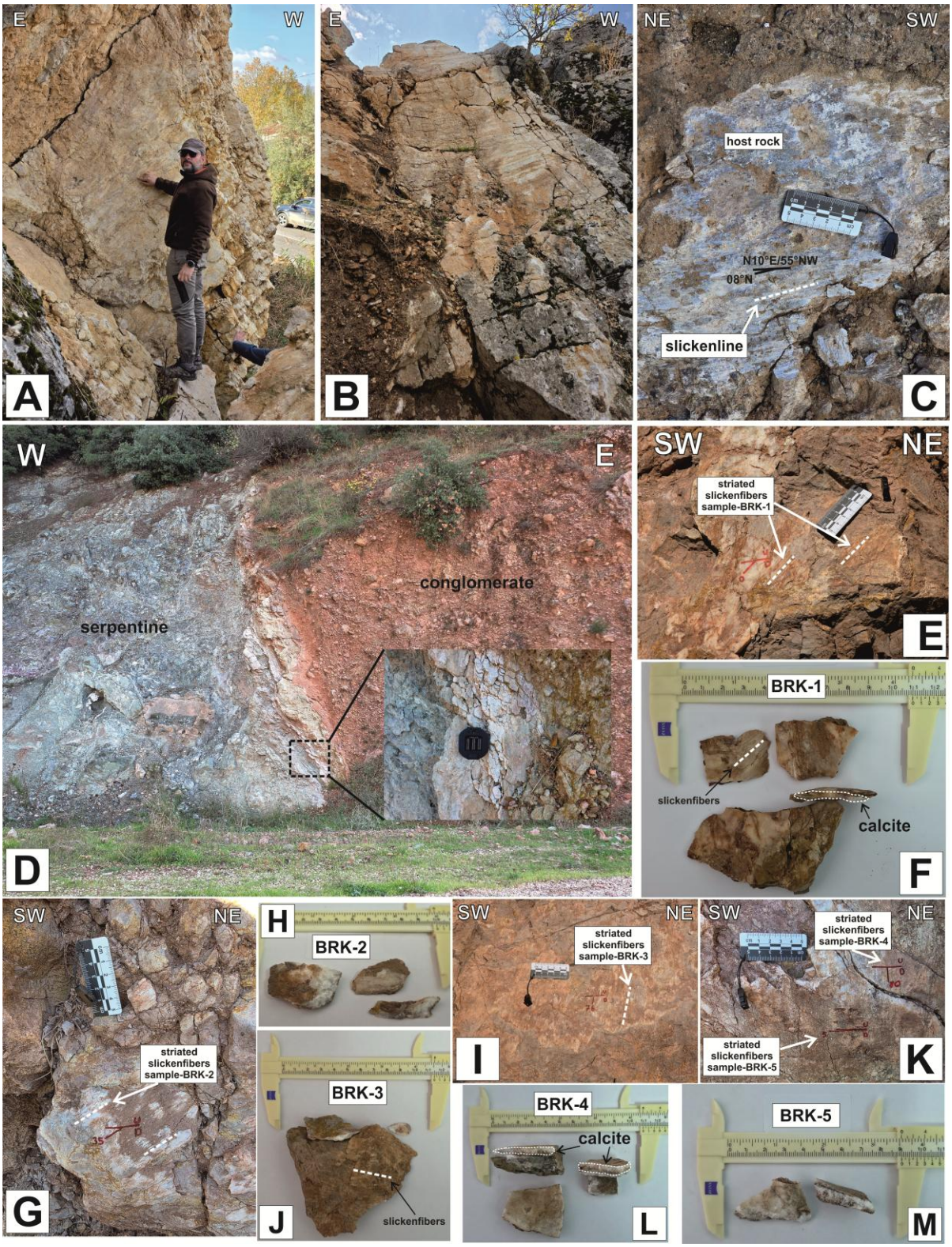

Supplementary Figure S1. Sampling photographs and structural context. Representative outcrop photographs illustrating the structural context of dated syntectonic carbonates along the EAF, including slickenfibres on slip surfaces, crack-seal/dilation veins, injection veins within gouge, and carbonate cement within breccias. Panels document sampling geometry and kinematic criteria used to link calcite growth to brittle deformation. (A-B) Pazarcık segment, Ozan location; (C) Pazarcık segment, Tevekkeli location; (D) Düziçi Fault, Burkaçlı location; (E-F) sample BRK-1, Burkaçlı location; (G-H) sample BRK-2, Burkaçlı location; (I-J) sample BRK-3, Burkaçlı location; (K-M) sample BRK-4 and BRK-5, Burkaçlı location

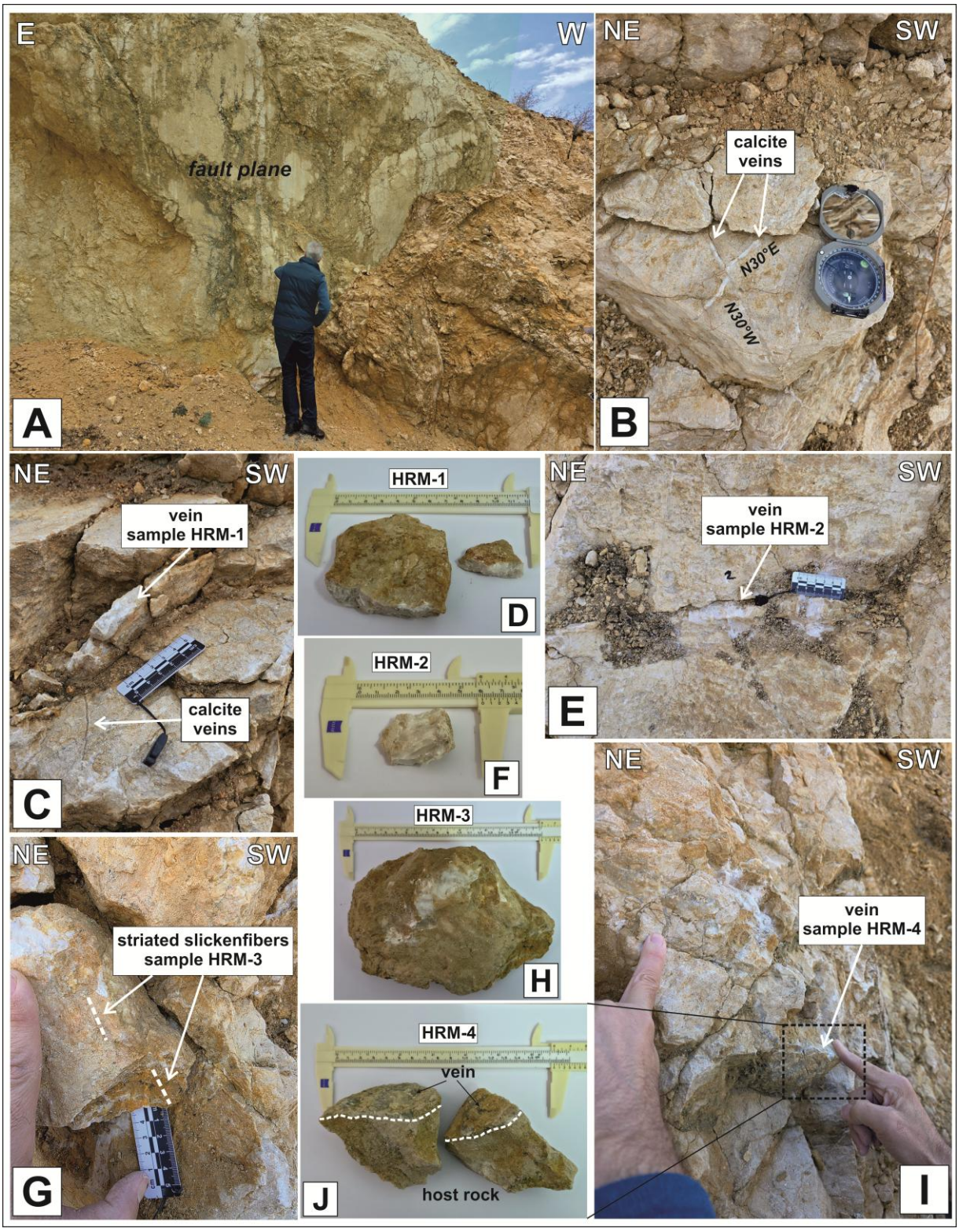

Supplementary Figure S2. Sampling photographs and structural context. Representative outcrop photographs illustrating the structural context of dated syntectonic carbonates along the EAF, including slickenfibres on slip surfaces, crack-seal/dilation veins, injection veins within gouge, and carbonate cement within breccias. Panels document sampling geometry and kinematic criteria used to link calcite growth to brittle deformation. (A-B) Erkenek segment, Harmanlı location; (C-D) sample HRM-1, Harmanlı location; (E-F-) sample HRM-2, Harmanlı location; (G-H) sample HRM-3, Harmanlı location; (J-I) sample HRM-4, Harmanlı location

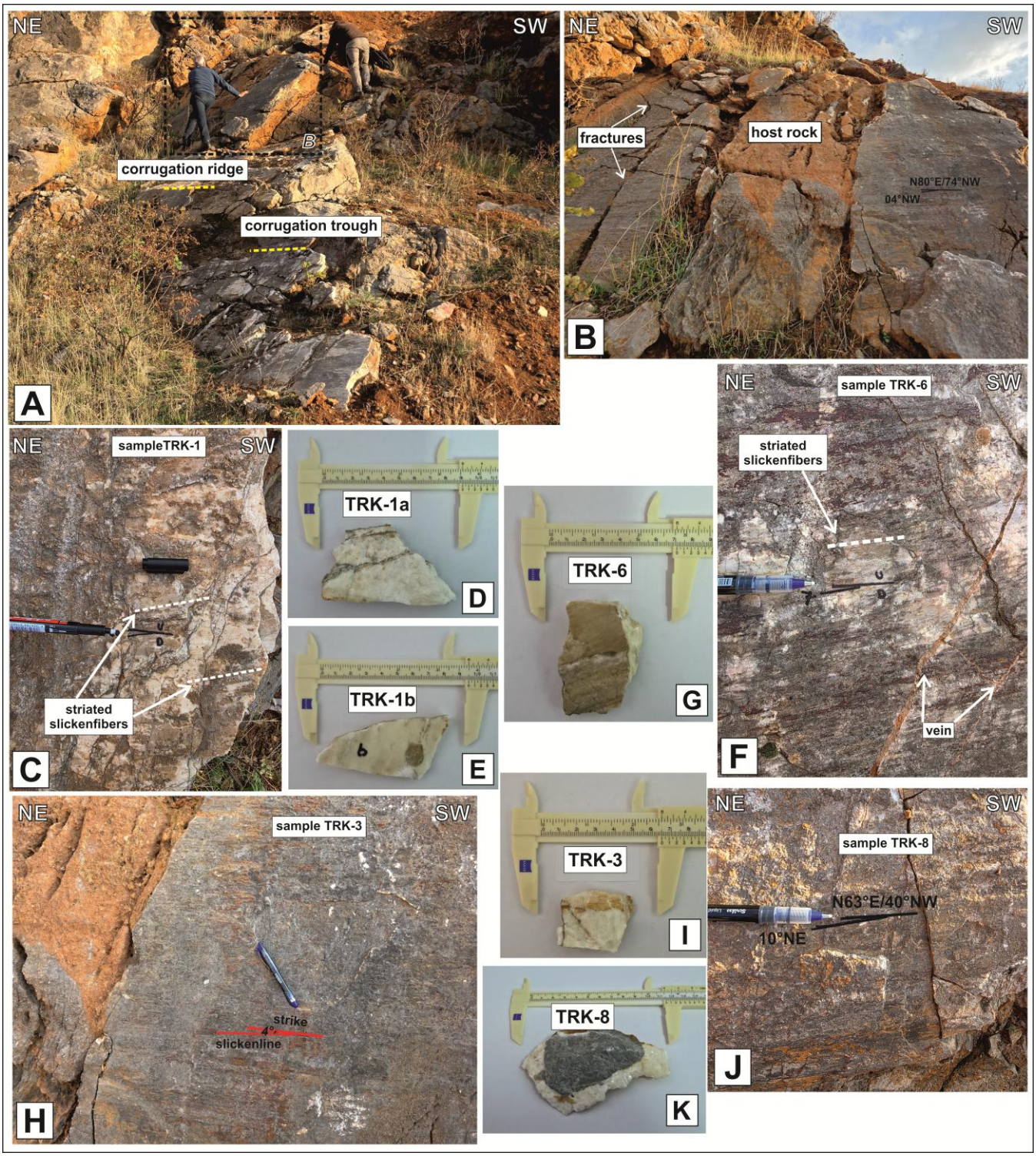

Supplementary Figure S3. Sampling photographs and structural context. Representative outcrop photographs illustrating the structural context of dated syntectonic carbonates along the EAF, including slickenfibres on slip surfaces, crack-seal/dilation veins, injection veins within gouge, and carbonate cement within breccias. Panels document sampling geometry and kinematic criteria used to link calcite growth to brittle deformation. (A-B) Pazarcık segment, Türkoğlu location; (C-E) sample TRK-1a and TRK-1b Türkoğlu location; (F-G) sample TRK-6, Türkoğlu location; (H-I) sample TRK-3, Türkoğlu location; (J-K) sample TRK-8, Türkoğlu location

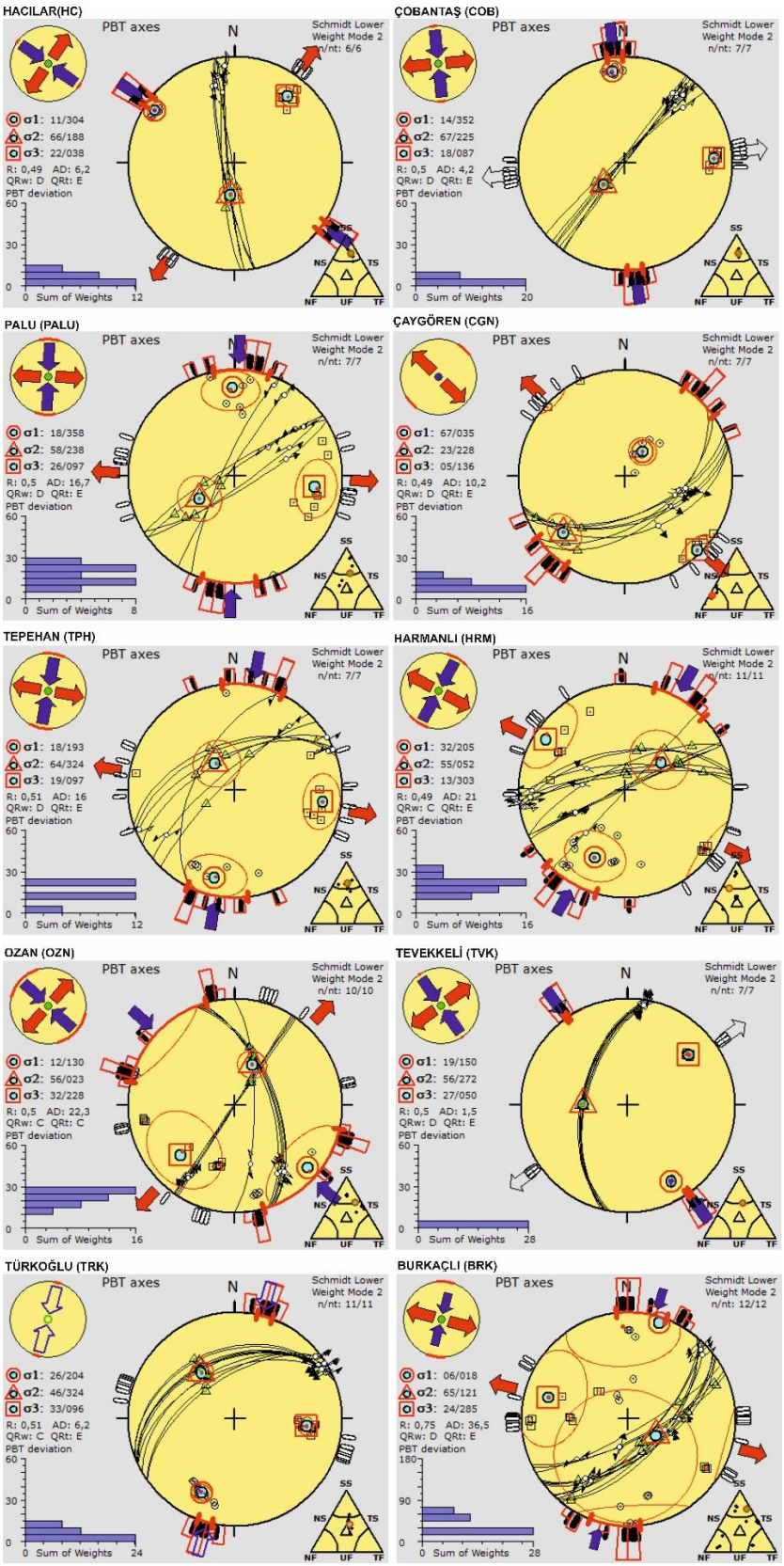

Supplementary Figure S4. Lower-hemisphere, equal area projection of paleostress orientations for each location.

Supplementary Table S6. Characteristics of stress states used to reconstruct stress regimes (Abbreviations: ϕ-ratio of stress magnitude differences (ϕ= (σ2- σ3) / (σ1- σ3); ANG- the average angle between observed slip and computed shear, in degrees; #-number of fault slip data)

Location	Fault orientations	Fault type	#	σ1	σ2	σ3	φ	ANG	Stress regime
HC	NW-SE	Left-lateral	7	11/304	66/188	22/038	0.490	6	Pure strike-slip
COB	NE-SW	Left-lateral	7	14/352	67/225	18/087	0.500	4	Pure strike-slip
PALU	NE-SW	Left-lateral	7	18/358	58/238	26/097	0.500	16	Pure strike-slip
CGN	NE-SW	Normal	7	67/035	23/228	05/136	0.490	10	Pure extension
TPH	NE-SW	Left-lateral	7	18/193	64/324	19/097	0.510	16	Pure strike-slip
HRM	NE-SW	Left-lateral	11	32/205	55/052	13/303	0.490	21	Pure strike-slip
OZN	NE-SW	Left-lateral	10	12/130	56/023	32/228	0.500	22	Pure strike-slip
TVK	NE-SW	Left-lateral	7	19/150	56/272	27/050	0.500	1	Pure strike-slip
TRK	NE-SW	Left-lateral	12	26/204	46/324	33/096	0.510	6	Pure strike-slip
BRK	NE-SW	Left-lateral	12	06/018	65/121	24/285	0.750	36	Pure strike-slip

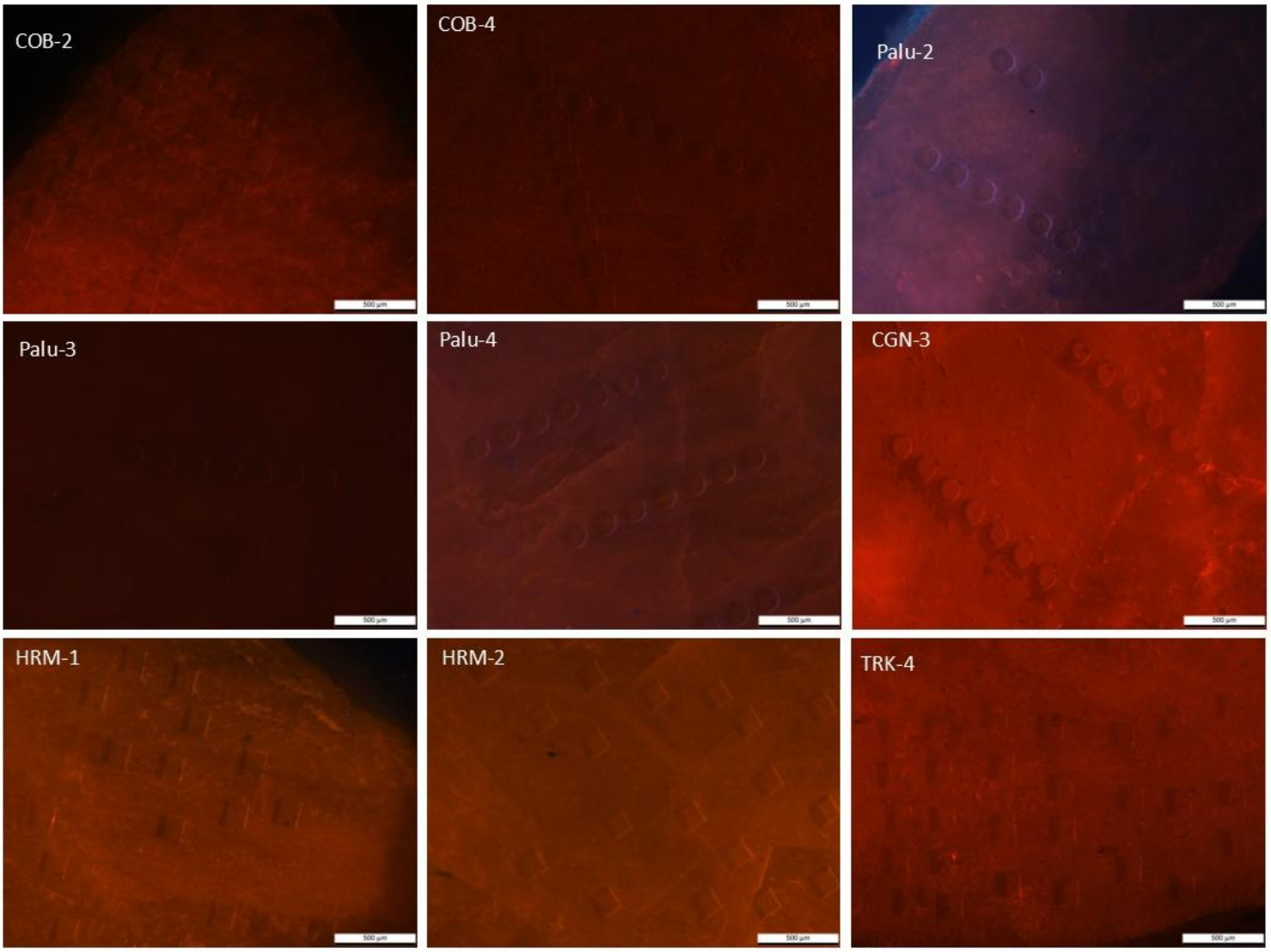

Supplementary Figure S5. Cathodoluminescence images showing locations of spot analyses within the calcite slickenfibres and veins. The homogeneity of colour observed in the CL image suggests that the sample has undergone little post-faulting alteration.

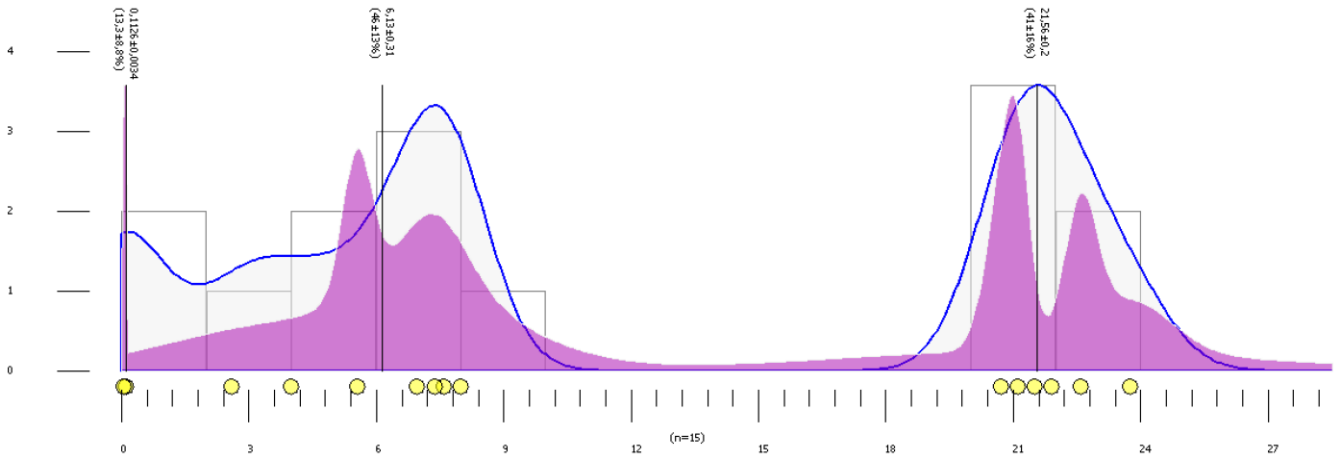

Supplementary Figure S6. Relative probability curve of the all U-Pb ages (10 samples, Supplementary Table S4). Note that the curve becomes sharper when the age errors (2 sigma) are smaller. Purple plot shows Probability Density Function (PDF) while turquoise plot shows Kernel Density Estimate (KDE). y-axis (sample number in 2 Ma of bin-width), x-axis (Ma).

Supplementary Table S7. LA-ICP-MS spot-by-spot dataset.

Spot	$^{238}U/^{206}Pb$	2s%	$^{207}Pb/^{206}Pb$	2s%	U (ppm)	Pb (ppm)
COB-2-1						
COB-2-1-1	0.016	0.001	0.815	0.006	0.036	7.613
COB-2-1-2	0.004	0.0002	0.810	0.006	0.013	11.869
COB-2-1-3	0.016	0.001	0.810	0.005	0.021	4.472
COB-2-1-4	0.050	0.003	0.818	0.008	0.022	1.501
COB-2-1-5	0.070	0.003	0.815	0.007	0.048	2.317
COB-2-1-6	0.063	0.002	0.807	0.007	0.048	2.565
COB-2-1-7	0.046	0.002	0.806	0.007	0.036	2.616
COB-2-1-8	0.199	0.008	0.815	0.009	0.072	1.226
COB-2-1-9	0.245	0.009	0.814	0.011	0.075	1.029
COB-2-1-10	0.288	0.011	0.807	0.010	0.130	1.495
COB-2-1-11	0.623	0.023	0.811	0.012	0.109	0.590
COB-2-1-12	0.609	0.034	0.799	0.019	0.037	0.201
COB-2-1-13	0.771	0.033	0.810	0.016	0.060	0.264
COB-2-1-14	1.917	0.078	0.825	0.033	0.054	0.096
COB-2-1-15	2.933	0.176	0.803	0.038	0.134	0.155
COB-2-1-16	2.892	0.159	0.814	0.020	0.137	0.158
COB-2-1-17	1.363	0.062	0.807	0.023	0.055	0.136
COB-2-1-18	1.043	0.056	0.809	0.021	0.077	0.249
COB-2-1-19	0.313	0.015	0.810	0.010	0.146	1.560
COB-2-1-20	0.557	0.024	0.813	0.015	0.109	0.658
COB-2-1-21	0.713	0.030	0.804	0.020	0.078	0.356
COB-2-1-22	0.012	0.001	0.820	0.008	0.007	1.975
COB-2-1-23	0.001	0.0001	0.818	0.004	0.004	14.402

COB-2-1-24	0.001	0.0001	0.821	0.003	0.006	14.172
COB-2-1-25	0.001	0.0001	0.820	0.003	0.005	15.559
COB-2-1-26	0.006	0.0003	0.816	0.005	0.009	5.272
COB-2-1-27	0.048	0.002	0.820	0.011	0.014	0.984
COB-2-1-28	0.042	0.002	0.804	0.007	0.051	4.009
COB-2-1-29	0.133	0.029	0.921	0.078	0.001	0.018
COB-2-1-30	1.065	0.047	0.818	0.015	0.161	0.503
COB-2-1-31	1.164	0.063	0.815	0.015	0.145	0.423
COB-2-1-32	0.703	0.043	0.812	0.012	0.120	0.572
COB-2-1-33	0.041	0.002	0.817	0.007	0.035	2.880
COB-2-1-34	0.004	0.0002	0.823	0.005	0.016	12.003
COB-2-1-35	0.006	0.0002	0.820	0.004	0.023	13.590
COB-2-1-36	0.004	0.0002	0.819	0.005	0.020	14.830
COB-2-1-37	0.017	0.001	0.812	0.010	0.037	7.246
COB-2-1-38	0.003	0.0001	0.818	0.006	0.009	11.812
COB-2-1-39	0.007	0.0003	0.817	0.008	0.023	11.484
COB-2-1-40	0.029	0.001	0.813	0.009	0.021	2.372
COB-2-1-41	0.060	0.003	0.824	0.015	0.029	1.670
COB-2-1-42	0.052	0.003	0.811	0.009	0.038	2.452
COB-2-1-43	0.028	0.002	0.817	0.009	0.011	1.312
COB-2-1-44	0.016	0.001	0.812	0.005	0.034	7.326
COB-2-1-45	0.013	0.001	0.813	0.005	0.032	8.384
COB-2-1-46	0.009	0.0004	0.813	0.007	0.019	7.128
COB-2-1-47	1.040	0.098	0.827	0.064	0.051	0.167
COB-2-1-48	2.199	0.107	0.832	0.027	0.067	0.100
COB-2-1-49	0.636	0.026	0.808	0.015	0.085	0.441
COB-2-1-50	0.534	0.023	0.805	0.014	0.109	0.680
COB-2-1-51	1.253	0.051	0.814	0.019	0.101	0.265
COB-2-1-52	2.422	0.120	0.841	0.031	0.052	0.076
COB-2-1-53	1.330	0.058	0.806	0.024	0.059	0.145
COB-2-1-54	117.318	5.506	0.712	0.024	13.237	0.338
COB-2-1-55	17.237	0.604	0.795	0.019	1.693	0.318
COB-2-1-56	1.187	0.048	0.818	0.016	0.100	0.281
COB-2-1-57	0.959	0.051	0.798	0.032	0.035	0.121
COB-2-1-58	0.729	0.040	0.802	0.021	0.056	0.257
COB-2-1-59	0.534	0.019	0.802	0.010	0.095	0.578
COB-2-1-60	1.443	0.060	0.814	0.014	0.163	0.381
COB-2-1-61	0.048	0.002	0.826	0.009	0.024	1.706
COB-2-1-62	0.043	0.002	0.816	0.010	0.014	1.110
COB-2-1-63	0.058	0.003	0.818	0.013	0.023	1.321
COB-2-1-64	0.023	0.001	0.804	0.009	0.040	5.861
COB-2-1-65	0.006	0.0002	0.821	0.005	0.018	10.710
COB-2-1-66	0.003	0.0002	0.821	0.004	0.009	10.442
COB-2-1-67	0.003	0.0001	0.819	0.005	0.011	11.843
COB-2-1-68	0.042	0.002	0.815	0.007	0.029	2.328

COB-2-1-69	0.051	0.002	0.819	0.007	0.026	1.725
COB-2-1-70	0.059	0.002	0.816	0.007	0.044	2.527
COB-2-1-71	0.059	0.003	0.815	0.008	0.043	2.430
COB-2-1-72	0.025	0.001	0.811	0.005	0.045	6.056
COB-2-1-73	0.030	0.001	0.814	0.005	0.047	5.260
COB-2-1-74	0.021	0.001	0.816	0.004	0.065	10.342
COB-2-1-75	0.005	0.0002	0.814	0.005	0.010	6.793
COB-2-1-76	0.003	0.0004	0.812	0.012	0.004	3.831
COB-2-1-77	0.003	0.0002	0.818	0.008	0.009	11.324
COB-2-1-78	0.045	0.002	0.812	0.008	0.040	2.993
COB-2-1-79	0.020	0.001	0.808	0.009	0.015	2.637
COB-2-1-80	0.017	0.001	0.821	0.009	0.015	2.896
COB-2-1-81	0.002	0.0001	0.823	0.006	0.009	12.495
COB-2-1-82	0.004	0.0002	0.820	0.005	0.013	11.900
COB-2-1-83	0.016	0.001	0.826	0.012	0.009	1.912
COB-2-1-84	0.028	0.001	0.825	0.008	0.011	1.323
COB-2-1-85	0.032	0.002	0.826	0.008	0.012	1.267
COB-2-1-86	0.052	0.003	0.819	0.014	0.017	1.107
COB-2-1-87	0.038	0.002	0.820	0.010	0.014	1.240
COB-2-1-88	0.070	0.003	0.814	0.011	0.013	0.622
COB-2-1-89	0.267	0.039	0.874	0.049	0.004	0.048
COB-2-1-90	0.580	0.051	0.810	0.021	0.086	0.504
COB-2-1-91	0.821	0.048	0.804	0.016	0.116	0.483
COB-2-1-92	0.418	0.018	0.798	0.017	0.053	0.416
COB-2-1-93	0.781	0.038	0.822	0.015	0.101	0.444
COB-2-1-94	0.419	0.017	0.812	0.012	0.078	0.624
COB-2-1-95	3.606	0.149	0.825	0.022	0.163	0.155
COB-2-1-96	3.311	0.131	0.806	0.020	0.269	0.268
COB-2-1-97	0.533	0.023	0.814	0.014	0.075	0.478
COB-2-1-98	0.295	0.017	0.808	0.012	0.103	1.173
COB-2-1-99	0.151	0.006	0.812	0.008	0.086	1.906
COB-2-1-100	0.099	0.004	0.812	0.008	0.061	2.075
COB-2-1-101	0.099	0.005	0.807	0.008	0.088	2.906
COB-2-2						
COB-2-2-1	0.315	0.006	0.804	0.010	0.289	2.703
COB-2-2-2	0.393	0.008	0.808	0.009	0.267	1.970
COB-2-2-3	0.418	0.009	0.804	0.011	0.237	1.676
COB-2-2-4	3.590	0.090	0.820	0.013	1.207	0.979
COB-2-2-5	36.919	0.516	0.773	0.012	19.838	1.487
COB-2-2-6	40.636	0.828	0.777	0.010	26.982	1.896
COB-2-2-7	68.229	2.283	0.756	0.009	48.245	1.919
COB-2-2-8	10.963	0.310	0.795	0.012	5.938	1.545
COB-2-2-9	62.206	1.364	0.752	0.010	39.957	1.712
COB-2-2-10	15.810	0.454	0.794	0.012	9.960	1.798
COB-2-2-11	15.752	0.488	0.789	0.012	7.728	1.424

COB-2-2-12	40.673	1.246	0.773	0.013	19.080	1.314
COB-2-2-13	25.114	0.390	0.798	0.012	11.903	1.366
COB-2-2-14	23.287	0.395	0.783	0.008	22.196	2.726
COB-2-2-15	117.876	1.814	0.714	0.016	32.929	0.717
COB-2-2-16	18.880	0.618	0.794	0.017	5.161	0.775
COB-2-2-17	1.220	0.023	0.809	0.015	0.503	1.215
COB-2-2-18	0.370	0.008	0.802	0.010	0.294	2.351
COB-2-2-19	0.272	0.005	0.810	0.009	0.272	2.985
COB-2-2-20	0.172	0.006	0.809	0.008	0.234	4.152
COB-2-2-21	0.277	0.008	0.802	0.017	0.262	2.868
COB-2-2-22	0.273	0.005	0.803	0.009	0.277	3.006
COB-2-2-23	0.318	0.006	0.810	0.008	0.361	3.405
COB-2-2-24	1.123	0.040	0.817	0.028	0.595	1.626
COB-2-2-25	0.510	0.011	0.804	0.010	0.359	2.130
COB-2-2-26	0.738	0.022	0.799	0.018	0.177	0.765
COB-2-2-27	0.792	0.026	0.810	0.019	0.155	0.594
COB-2-2-28	1.278	0.036	0.812	0.018	0.334	0.776
COB-2-2-29	2.231	0.065	0.828	0.016	0.666	0.906
COB-2-2-30	15.459	0.417	0.788	0.015	5.190	0.974
COB-2-2-31	1.184	0.028	0.810	0.013	0.439	1.118
COB-2-2-32	1.222	0.053	0.811	0.023	0.244	0.588
COB-2-2-33	2.248	0.127	0.820	0.013	1.031	1.356
COB-2-2-34	1.151	0.021	0.800	0.019	0.657	1.682
COB-2-2-35	0.322	0.006	0.803	0.010	0.257	2.373
COB-2-2-36	0.311	0.009	0.808	0.010	0.266	2.548
COB-2-2-37	0.189	0.004	0.806	0.007	0.344	5.395
COB-2-2-38	0.250	0.005	0.806	0.008	0.409	4.827
COB-2-2-39	0.177	0.006	0.811	0.009	0.234	3.938
COB-2-2-40	0.267	0.006	0.812	0.009	0.311	3.452
COB-2-2-41	0.327	0.006	0.812	0.009	0.408	3.694
COB-2-2-42	0.252	0.006	0.804	0.021	0.529	6.089
COB-2-2-43	0.215	0.005	0.807	0.006	0.475	6.484
COB-2-2-44	0.199	0.003	0.810	0.007	0.416	6.218
COB-2-2-45	0.215	0.004	0.803	0.007	0.441	6.052
COB-2-2-46	0.273	0.006	0.813	0.007	0.548	5.979
COB-2-2-47	0.380	0.006	0.808	0.008	0.599	4.680
COB-2-2-48	0.280	0.009	0.805	0.008	0.503	5.308
COB-2-2-49	0.301	0.009	0.799	0.008	0.474	4.623
COB-2-2-50	0.484	0.010	0.802	0.010	0.579	3.580
COB-2-2-51	0.262	0.004	0.807	0.007	0.503	5.710
COB-2-2-52	0.218	0.003	0.806	0.006	0.616	8.433
COB-2-2-53	0.258	0.005	0.807	0.009	0.290	3.361
COB-2-2-54	1.029	0.042	0.818	0.015	0.492	1.458
COB-2-2-55	0.408	0.009	0.804	0.013	0.233	1.712
COB-2-2-56	0.117	0.002	0.807	0.007	0.221	5.538

COB-2-2-57	0.059	0.001	0.805	0.005	0.264	13.295
COB-2-2-58	0.189	0.005	0.803	0.013	0.269	4.144
COB-2-2-59	0.331	0.008	0.812	0.008	0.409	3.698
COB-2-2-60	1.050	0.026	0.820	0.020	0.236	0.679
COB-2-2-61	2.556	0.082	0.809	0.034	0.262	0.295
COB-2-2-62	1.125	0.044	0.806	0.020	0.262	0.693
COB-2-2-63	0.421	0.013	0.794	0.014	0.319	2.178
COB-2-2-64	0.213	0.004	0.805	0.008	0.373	5.166
COB-2-2-65	0.283	0.005	0.796	0.010	0.262	2.698
COB-2-2-66	0.926	0.022	0.815	0.017	0.363	1.160
COB-2-2-67	0.254	0.006	0.807	0.008	0.437	5.125
COB-2-2-68	0.615	0.011	0.804	0.010	0.592	2.786
COB-2-2-69	0.363	0.008	0.795	0.009	0.575	4.633
COB-2-2-70	0.726	0.012	0.806	0.012	0.405	1.639
COB-2-2-71	1.603	0.047	0.798	0.024	0.236	0.424
COB-2-2-72	1.058	0.035	0.813	0.023	0.160	0.467
COB-2-2-73	2.364	0.061	0.820	0.025	0.310	0.388
COB-2-2-74	0.903	0.026	0.817	0.023	0.143	0.462
COB-2-2-75	0.355	0.010	0.811	0.014	0.171	1.438
COB-2-2-76	0.934	0.028	0.810	0.018	0.241	0.769
COB-2-2-77	0.573	0.012	0.814	0.016	0.185	0.962
COB-2-2-78	0.129	0.004	0.803	0.010	0.172	3.943
COB-2-2-79	0.190	0.004	0.806	0.012	0.154	2.370
COB-2-2-80	0.179	0.004	0.793	0.014	0.120	1.976
COB-2-2-81	0.592	0.012	0.814	0.017	0.166	0.843
COB-2-2-82	0.317	0.009	0.816	0.018	0.125	1.196
COB-2-2-83	0.959	0.018	0.820	0.016	0.234	0.735
COB-2-2-84	0.788	0.039	0.813	0.019	0.188	0.733
COB-2-2-85	0.735	0.016	0.817	0.019	0.134	0.552
COB-2-2-86	0.896	0.022	0.806	0.014	0.258	0.859
COB-2-2-87	0.598	0.013	0.808	0.017	0.157	0.770
COB-2-2-88	0.215	0.004	0.802	0.008	0.238	3.279
COB-2-2-89	0.180	0.004	0.805	0.006	0.299	4.940
COB-2-2-90	0.247	0.006	0.809	0.008	0.344	4.170
COB-2-2-91	0.314	0.005	0.815	0.009	0.326	3.097
COB-2-2-92	0.217	0.004	0.805	0.008	0.237	3.179
COB-2-2-93	0.120	0.003	0.803	0.008	0.191	4.722
COB-2-2-94	0.196	0.003	0.802	0.006	0.281	4.249
COB-2-2-95	0.081	0.002	0.803	0.007	0.118	4.324
COB-2-2-96	0.074	0.001	0.800	0.006	0.137	5.447
COB-2-2-97	0.114	0.002	0.812	0.008	0.167	4.346
COB-2-2-98	0.300	0.004	0.803	0.009	0.316	3.115
COB-4a						
COB-4a-1	0.122	0.011	0.813	0.021	0.069	1.868
COB-4a-2	0.111	0.006	0.813	0.014	0.061	1.808

COB-4a-3	0.128	0.007	0.814	0.017	0.081	2.072
COB-4a-4	0.109	0.006	0.817	0.011	0.075	2.245
COB-4a-5	0.091	0.007	0.816	0.013	0.051	1.869
COB-4a-6	0.199	0.012	0.817	0.016	0.121	2.030
COB-4a-7	0.185	0.009	0.808	0.012	0.079	1.418
COB-4a-8	0.087	0.004	0.816	0.008	0.082	3.124
COB-4a-9	0.273	0.014	0.811	0.008	0.144	1.749
COB-4a-10	1.678	0.068	0.806	0.008	0.557	1.088
COB-4a-11	0.139	0.007	0.810	0.006	0.101	2.408
COB-4a-12	0.112	0.006	0.806	0.006	0.081	2.388
COB-4a-13	0.081	0.004	0.817	0.007	0.065	2.624
COB-4a-14	0.312	0.020	0.810	0.006	0.288	3.073
COB-4a-15	0.077	0.003	0.815	0.006	0.060	2.612
COB-4a-16	0.136	0.006	0.812	0.006	0.095	2.327
COB-4a-17	0.051	0.002	0.810	0.007	0.050	3.255
COB-4a-18	0.102	0.005	0.820	0.008	0.130	4.210
COB-4a-19	0.042	0.002	0.813	0.007	0.043	3.388
COB-4a-20	0.076	0.004	0.813	0.005	0.096	4.170
COB-4a-21	0.109	0.005	0.810	0.007	0.104	3.156
COB-4a-22	0.182	0.008	0.814	0.009	0.119	2.193
COB-4a-23	0.276	0.013	0.813	0.008	0.172	2.082
COB-4a-24	0.177	0.011	0.818	0.008	0.094	1.783
COB-4a-25	0.162	0.008	0.814	0.009	0.103	2.109
COB-4a-26	0.161	0.007	0.808	0.008	0.090	1.846
COB-4a-27	0.279	0.015	0.815	0.010	0.160	1.910
COB-4a-28	0.199	0.009	0.812	0.008	0.086	1.428
COB-4a-29	0.348	0.016	0.803	0.010	0.137	1.305
COB-4a-30	3.108	0.135	0.793	0.009	0.956	1.007
COB-4a-31	0.272	0.020	0.814	0.012	0.112	1.388
COB-4a-32	0.413	0.020	0.804	0.011	0.112	0.893
COB-4a-33	3.674	0.161	0.807	0.007	1.778	1.594
COB-4a-34	0.979	0.048	0.808	0.009	0.257	0.881
COB-4a-35	1.356	0.061	0.810	0.013	0.242	0.588
COB-4a-36	0.241	0.011	0.808	0.008	0.146	1.996
COB-4a-37	0.193	0.009	0.810	0.008	0.110	1.891
COB-4a-38	0.250	0.011	0.813	0.007	0.133	1.775
COB-4a-39	0.254	0.011	0.821	0.009	0.112	1.469
COB-4a-40	0.213	0.009	0.809	0.010	0.079	1.223
COB-4a-41	0.294	0.014	0.805	0.009	0.103	1.160
COB-4a-42	0.248	0.015	0.814	0.014	0.073	0.973
COB-4a-43	0.554	0.030	0.803	0.010	0.105	0.621
COB-4a-44	0.517	0.023	0.802	0.013	0.108	0.690
COB-4a-45	0.210	0.010	0.805	0.012	0.064	1.012
COB-4a-46	0.328	0.015	0.815	0.011	0.073	0.746
COB-4a-47	0.209	0.010	0.805	0.010	0.053	0.839

COB-4a-48	0.185	0.009	0.812	0.008	0.075	1.343
COB-4a-49	0.167	0.009	0.813	0.008	0.058	1.149
COB-4a-50	0.176	0.009	0.807	0.008	0.071	1.342
COB-4a-51	0.101	0.006	0.825	0.014	0.043	1.420
COB-4a-52	0.176	0.009	0.811	0.013	0.076	1.442
COB-4a-53	0.241	0.011	0.805	0.012	0.058	0.801
COB-4a-54	0.255	0.013	0.817	0.018	0.055	0.726
COB-4a-55	0.334	0.015	0.810	0.011	0.143	1.435
COB-4a-56	0.700	0.040	0.804	0.010	0.163	0.767
COB-4a-57	4.648	0.201	0.764	0.020	0.680	0.466
COB-4a-58	0.090	0.005	0.809	0.012	0.042	1.563
COB-4a-59	0.165	0.007	0.817	0.008	0.112	2.250
COB-4a-60	0.100	0.006	0.812	0.006	0.083	2.720
COB-4a-61	0.117	0.006	0.805	0.009	0.107	3.021
COB-4a-62	0.189	0.009	0.810	0.008	0.079	1.401
COB-4a-63	0.287	0.014	0.824	0.012	0.084	0.985
COB-4a-64	0.341	0.017	0.808	0.012	0.107	1.061
COB-4a-65	0.575	0.030	0.806	0.010	0.157	0.928
COB-4a-66	0.320	0.014	0.809	0.009	0.151	1.612
COB-4a-67	0.240	0.011	0.812	0.009	0.109	1.529
COB-4a-68	0.485	0.024	0.815	0.009	0.288	2.008
COB-4a-69	0.481	0.026	0.811	0.008	0.293	2.050
COB-4a-70	0.177	0.009	0.814	0.013	0.057	1.087
COB-4a-71	0.259	0.012	0.805	0.010	0.067	0.878
COB-4a-72	1.770	0.093	0.802	0.010	0.574	1.078
COB-4a-73	27.457	1.194	0.716	0.015	4.046	0.442
COB-4a-74	1.638	0.078	0.799	0.012	0.308	0.633
COB-4a-75	0.378	0.032	0.819	0.032	0.076	0.688
COB-4a-76	0.419	0.025	0.801	0.024	0.049	0.382
COB-4a-77	0.438	0.027	0.814	0.020	0.041	0.320
COB-4a-78	1.265	0.077	0.808	0.028	0.068	0.177
COB-4a-79	0.054	0.003	0.811	0.012	0.041	2.446
COB-4a-80	0.089	0.005	0.817	0.017	0.067	2.573
COB-4a-81	0.180	0.013	0.818	0.015	0.135	2.435
COB-4a-82	0.088	0.004	0.808	0.011	0.100	3.755
COB-4a-83	0.237	0.009	0.808	0.009	0.215	2.926
COB-4a-84	0.350	0.021	0.806	0.009	0.277	2.582
COB-4a-85	0.223	0.009	0.810	0.010	0.213	3.094
COB-4a-86	0.482	0.021	0.807	0.013	0.088	0.595
COB-4a-87	0.502	0.024	0.807	0.013	0.091	0.593
COB-4a-88	0.520	0.025	0.815	0.013	0.082	0.525
COB-4a-89	7.630	0.331	0.804	0.011	1.803	0.781
COB-4a-90	2.000	0.094	0.815	0.014	0.306	0.501
COB-4a-91	0.597	0.025	0.813	0.013	0.111	0.620
COB-4a-92	0.891	0.046	0.823	0.021	0.088	0.333

COB-4a-93	0.350	0.020	0.832	0.030	0.068	0.679
COB-4a-94	0.429	0.026	0.829	0.022	0.057	0.454
COB-4a-95	0.557	0.032	0.807	0.018	0.078	0.459
COB-4a-96	15.163	0.627	0.807	0.013	2.645	0.581
COB-4a-97	0.435	0.020	0.815	0.016	0.096	0.745
COB-4a-98	1.343	0.064	0.820	0.021	0.109	0.273
COB-4a-99	0.783	0.038	0.805	0.016	0.076	0.319
COB-4a-100	0.306	0.014	0.808	0.009	0.125	1.351
COB-4a-101	0.189	0.009	0.812	0.009	0.133	2.317
COB-4a-102	0.203	0.011	0.814	0.009	0.102	1.647
COB-4a-103	0.177	0.008	0.807	0.007	0.112	2.076
COB-4a-104	0.836	0.036	0.810	0.012	0.218	0.873
COB-4a-105	3.577	0.158	0.799	0.012	0.998	0.901
COB-4a-106	0.582	0.031	0.810	0.009	0.201	1.153
COB-4b-1						
COB-4b-1-1	32.77	1.196	0.765	0.021	0.840	0.080
COB-4b-1-2	25.37	1.142	0.759	0.020	0.785	0.098
COB-4b-1-3	18.37	0.913	0.753	0.018	1.041	0.176
COB-4b-1-4	16.97	0.658	0.749	0.017	0.736	0.135
COB-4b-1-5	7.65	0.339	0.791	0.016	0.363	0.152
COB-4b-1-6	9.75	0.451	0.781	0.020	0.451	0.150
COB-4b-1-7	4.38	0.155	0.784	0.016	0.239	0.175
COB-4b-1-8	16.74	0.702	0.785	0.020	0.546	0.102
COB-4b-1-9	41.97	3.791	0.760	0.029	0.995	0.091
COB-4b-1-10	20.50	0.796	0.780	0.024	0.535	0.086
COB-4b-1-11	25.00	1.222	0.785	0.026	0.502	0.064
COB-4b-1-12	18.38	0.736	0.766	0.027	0.338	0.058
COB-4b-1-13	10.50	0.422	0.784	0.023	0.306	0.095
COB-4b-1-14	11.67	0.500	0.785	0.025	0.329	0.089
COB-4b-1-15	4.30	0.189	0.778	0.012	0.396	0.300
COB-4b-1-16	5.52	0.234	0.772	0.016	0.437	0.255
COB-4b-1-17	3.48	0.141	0.793	0.016	0.260	0.242
COB-4b-1-18	4.60	0.166	0.779	0.014	0.332	0.234
COB-4b-1-19	3.11	0.126	0.794	0.017	0.294	0.310
COB-4b-1-20	4.37	0.146	0.770	0.018	0.297	0.216
COB-4b-1-21	24.00	0.910	0.778	0.028	0.410	0.054
COB-4b-1-22	44.76	1.947	0.773	0.023	0.882	0.062
COB-4b-1-23	21.37	0.858	0.787	0.024	0.560	0.084
COB-4b-1-24	30.88	1.584	0.758	0.027	0.630	0.062
COB-4b-1-25	33.06	1.285	0.775	0.022	0.977	0.095
COB-4b-1-26	14.39	0.563	0.782	0.017	0.612	0.137
COB-4b-1-27	4.10	0.262	0.810	0.012	0.685	0.581
COB-4b-1-28	33.39	1.451	0.752	0.023	0.513	0.048
COB-4b-1-29	35.07	1.597	0.757	0.036	0.476	0.042
COB-4b-1-30	10.04	0.484	0.787	0.023	0.224	0.072

COB-4b-1-31	7.03	0.279	0.762	0.024	0.157	0.072
COB-4b-1-32	35.91	1.653	0.758	0.024	0.730	0.062
COB-4b-1-33	13.84	0.654	0.777	0.022	0.394	0.093
COB-4b-1-34	21.92	0.969	0.750	0.032	0.356	0.050
COB-4b-1-35	24.16	1.015	0.732	0.026	0.392	0.049
COB-4b-1-36	37.16	1.623	0.768	0.027	0.634	0.054
COB-4b-1-37	17.93	0.723	0.778	0.023	0.463	0.079
COB-4b-1-38	17.47	0.756	0.766	0.027	0.371	0.068
COB-4b-1-39	25.83	1.025	0.744	0.027	0.507	0.064
COB-4b-1-40	35.42	1.472	0.772	0.026	0.744	0.064
COB-4b-1-41	33.07	1.997	0.786	0.030	0.697	0.070
COB-4b-1-42	28.52	1.231	0.731	0.028	0.535	0.055
COB-4b-1-43	28.00	1.290	0.762	0.022	0.542	0.062
COB-4b-1-44	30.30	1.401	0.776	0.036	0.461	0.046
COB-4b-1-45	14.89	0.591	0.770	0.023	0.381	0.081
COB-4b-1-46	21.52	0.929	0.796	0.024	0.520	0.080
COB-4b-1-47	17.28	0.736	0.788	0.019	0.566	0.107
COB-4b-1-48	15.18	0.718	0.791	0.026	0.361	0.076
COB-4b-1-49	38.00	1.502	0.790	0.012	5.163	0.435
COB-4b-1-50	1.60	0.075	0.795	0.011	0.193	0.403
COB-4b-1-51	0.83	0.032	0.805	0.010	0.097	0.393
COB-4b-1-52	3.15	0.127	0.798	0.011	0.316	0.334
COB-4b-1-53	1.49	0.054	0.795	0.011	0.151	0.328
COB-4b-1-54	1.28	0.054	0.816	0.012	0.163	0.429
COB-4b-1-55	1.58	0.057	0.809	0.011	0.175	0.368
COB-4b-1-56	40.16	1.655	0.757	0.022	0.935	0.076
COB-4b-1-57	55.62	2.627	0.776	0.034	1.868	0.107
COB-4b-1-58	63.37	3.288	0.784	0.034	1.475	0.073
COB-4b-1-59	36.22	1.624	0.771	0.034	0.842	0.069
COB-4b-1-60	73.94	3.485	0.710	0.037	1.059	0.041
COB-4b-1-61	43.19	1.698	0.757	0.024	0.849	0.059
COB-4b-1-62	52.32	2.183	0.783	0.034	0.994	0.060
COB-4b-1-63	3.77	0.458	0.805	0.009	0.867	0.892
COB-4b-1-64	8.83	0.433	0.806	0.011	2.327	0.884
COB-4b-1-65	3.32	0.224	0.820	0.009	0.651	0.684
COB-4b-1-66	5.12	0.214	0.818	0.013	0.957	0.622
COB-4b-1-67	4.07	0.173	0.799	0.011	0.776	0.628
COB-4b-1-68	3.54	0.140	0.811	0.011	0.714	0.677
COB-4b-1-69	1.30	0.091	0.800	0.011	0.184	0.468
COB-4b-1-70	2.60	0.154	0.807	0.012	0.447	0.579
COB-4b-1-71	1.35	0.057	0.800	0.012	0.534	1.292
COB-4b-1-72	7.87	0.309	0.798	0.016	0.467	0.194
COB-4b-1-73	6.92	0.456	0.774	0.017	0.450	0.221
COB-4b-1-74	0.25	0.013	0.806	0.007	0.331	4.474
COB-4b-1-75	1.61	0.073	0.806	0.010	0.323	0.670

COB-4b-1-76	0.81	0.036	0.795	0.015	0.205	0.852
COB-4b-1-77	6.80	0.848	0.774	0.023	0.367	0.226
COB-4b-1-78	7.67	0.326	0.771	0.018	0.278	0.114
COB-4b-1-79	11.14	0.492	0.777	0.021	0.495	0.143
COB-4b-1-80	16.14	1.044	0.814	0.024	0.767	0.162
COB-4b-1-81	4.19	0.153	0.759	0.016	0.398	0.300
COB-4b-1-82	3.63	0.178	0.794	0.022	0.266	0.240
COB-4b-1-83	3.54	0.147	0.811	0.016	0.249	0.233
COB-4b-1-84	6.92	0.302	0.773	0.020	0.271	0.120
COB-4b-1-85	8.32	0.337	0.780	0.018	0.420	0.165
COB-4b-1-86	11.31	0.476	0.779	0.019	0.379	0.105
COB-4b-1-87	26.71	1.197	0.771	0.032	0.472	0.056
COB-4b-1-88	17.31	0.715	0.757	0.025	0.387	0.071
COB-4b-1-89	40.69	1.717	0.770	0.025	0.962	0.075
COB-4b-1-90	62.30	2.652	0.764	0.028	1.061	0.055
COB-4b-1-91	43.00	1.955	0.799	0.030	0.731	0.054
COB-4b-1-92	27.10	1.163	0.764	0.025	0.596	0.070
COB-4b-1-93	44.42	1.863	0.757	0.025	0.817	0.059
COB-4b-1-94	42.98	1.812	0.745	0.026	0.728	0.053
COB-4b-1-95	47.23	1.966	0.747	0.029	0.861	0.057
COB-4b-1-96	21.83	1.062	0.804	0.030	0.422	0.064
COB-4b-1-97	42.25	2.174	0.771	0.035	0.678	0.051
COB-4b-1-98	78.96	3.710	0.741	0.032	1.243	0.047
COB-4b-1-99	34.31	1.334	0.750	0.023	0.739	0.067
COB-4b-1-100	31.83	1.315	0.766	0.029	0.754	0.069
COB-4b-1-101	10.06	0.485	0.812	0.029	0.214	0.071
COB-4b-1-102	24.59	1.068	0.802	0.030	0.540	0.070
COB-4b-1-103	47.898	1.329	0.760	0.030	2.601	0.142
COB-4b-2						
COB-4b-2-2	30.697	0.864	0.775	0.028	2.246	0.198
COB-4b-2-3	33.082	1.017	0.752	0.031	1.833	0.143
COB-4b-2-4	52.505	1.931	0.751	0.034	2.468	0.133
COB-4b-2-5	26.697	0.743	0.788	0.029	1.870	0.187
COB-4b-2-6	46.308	1.464	0.775	0.036	3.038	0.176
COB-4b-2-7	89.435	3.228	0.731	0.031	5.047	0.150
COB-4b-2-8	75.555	2.691	0.769	0.039	3.999	0.141
COB-4b-2-9	48.307	1.781	0.742	0.029	3.221	0.182
COB-4b-2-10	9.392	0.263	0.772	0.030	1.258	0.363
COB-4b-2-11	52.195	1.588	0.745	0.030	4.040	0.201
COB-4b-2-12	32.550	0.682	0.761	0.031	2.692	0.227
COB-4b-2-13	34.658	0.764	0.754	0.027	3.984	0.296
COB-4b-2-14	36.809	1.158	0.769	0.027	2.849	0.217
COB-4b-2-15	3.693	0.170	0.797	0.010	2.449	2.012
COB-4b-2-16	1.225	0.053	0.802	0.008	2.281	5.632
COB-4b-2-17	48.455	1.590	0.758	0.030	2.992	0.168

COB-4b-2-18	37.203	0.977	0.745	0.023	3.059	0.231
COB-4b-2-19	16.483	0.551	0.797	0.026	1.592	0.274
COB-4b-2-20	55.105	2.035	0.746	0.031	2.883	0.148
COB-4b-2-21	25.058	0.623	0.783	0.022	1.845	0.204
COB-4b-2-22	26.932	0.769	0.760	0.028	2.021	0.213
COB-4b-2-23	13.811	0.377	0.777	0.030	0.979	0.193
COB-4b-2-24	31.641	0.838	0.750	0.027	2.491	0.217
COB-4b-2-25	15.304	0.351	0.791	0.026	1.548	0.301
COB-4b-2-26	36.278	1.011	0.740	0.022	2.642	0.207
COB-4b-2-27	37.097	1.250	0.779	0.031	2.290	0.176
COB-4b-2-28	37.693	0.988	0.773	0.031	2.435	0.178
COB-4b-2-29	22.786	0.502	0.782	0.026	2.203	0.270
COB-4b-2-30	48.635	1.849	0.757	0.033	2.982	0.167
COB-4b-2-31	55.295	1.732	0.771	0.030	3.995	0.200
COB-4b-2-32	69.316	2.295	0.739	0.027	4.699	0.184
COB-4b-2-33	72.283	2.174	0.753	0.035	4.251	0.154
COB-4b-2-34	51.799	1.798	0.767	0.029	3.917	0.207
COB-4b-2-35	39.393	2.561	0.737	0.051	2.879	0.196
COB-4b-2-36	93.052	3.891	0.729	0.032	4.815	0.131
COB-4b-2-37	109.491	3.801	0.762	0.034	5.667	0.131
COB-4b-2-38	31.259	0.982	0.761	0.028	2.546	0.229
COB-4b-2-39	52.092	1.464	0.749	0.030	3.707	0.192
COB-4b-2-40	57.260	1.996	0.719	0.026	3.351	0.148
COB-4b-2-41	33.207	0.959	0.785	0.033	2.804	0.232
COB-4b-2-42	34.245	1.092	0.767	0.029	2.314	0.187
COB-4b-2-43	19.770	0.457	0.774	0.026	2.016	0.274
COB-4b-2-44	17.434	0.496	0.785	0.034	1.175	0.188
COB-4b-2-45	24.934	0.646	0.771	0.028	2.014	0.224
COB-4b-2-46	36.629	1.063	0.739	0.030	2.282	0.167
COB-4b-2-47	16.134	0.789	0.755	0.032	1.899	0.320
COB-4b-2-48	22.717	0.761	0.803	0.035	2.300	0.294
COB-4b-2-49	22.197	0.969	0.800	0.052	1.597	0.207
COB-4b-2-50	44.368	1.563	0.752	0.034	2.684	0.165
COB-4b-2-51	29.772	0.746	0.767	0.029	2.096	0.192
COB-4b-2-52	9.928	0.434	0.787	0.044	1.009	0.300
COB-4b-2-53	10.215	0.251	0.762	0.026	0.925	0.249
COB-4b-2-54	26.890	1.194	0.754	0.026	2.017	0.218
COB-4b-2-55	0.671	0.018	0.788	0.014	0.253	1.095
COB-4b-2-56	1.255	0.026	0.812	0.014	0.517	1.215
COB-4b-2-57	1.842	0.043	0.798	0.015	0.707	1.117
COB-4b-2-58	1.110	0.018	0.775	0.011	0.447	1.143
COB-4b-2-59	0.728	0.018	0.787	0.017	0.275	1.085
COB-4b-2-60	0.958	0.016	0.793	0.013	0.369	1.123
COB-4b-2-61	0.615	0.017	0.813	0.018	0.190	0.899
COB-4b-2-62	0.761	0.018	0.806	0.015	0.273	1.055

COB-4b-2-63	0.930	0.023	0.822	0.035	0.330	1.017
COB-4b-2-64	0.884	0.015	0.793	0.015	0.302	0.974
COB-4b-2-65	1.164	0.027	0.793	0.016	0.379	0.943
COB-4b-2-66	1.515	0.044	0.797	0.016	0.474	0.887
COB-4b-2-67	2.210	0.056	0.814	0.017	0.670	0.880
COB-4b-2-68	0.973	0.035	0.798	0.028	0.318	0.985
COB-4b-2-69	0.930	0.020	0.789	0.016	0.302	0.927
COB-4b-2-70	1.193	0.022	0.795	0.014	0.307	0.739
COB-4b-2-71	0.538	0.023	0.784	0.017	0.129	0.684
COB-4b-2-72	1.012	0.035	0.789	0.014	0.351	0.989
COB-4b-2-73	0.762	0.022	0.782	0.026	0.308	1.164
COB-4b-2-74	0.630	0.015	0.781	0.014	0.187	0.840
COB-4b-2-75	1.253	0.051	0.786	0.013	0.338	0.777
COB-4b-2-76	1.171	0.021	0.797	0.013	0.400	0.994
COB-4b-2-77	1.815	0.038	0.791	0.016	0.526	0.838
COB-4b-2-78	1.790	0.051	0.780	0.015	0.622	0.999
COB-4b-2-79	0.997	0.016	0.782	0.020	0.326	0.938
COB-4b-2-80	1.068	0.021	0.788	0.014	0.363	0.964
COB-4b-2-81	1.158	0.023	0.791	0.013	0.392	0.976
COB-4b-2-82	1.343	0.031	0.801	0.015	0.422	0.893
COB-4b-2-83	0.671	0.016	0.793	0.017	0.222	0.931
COB-4b-2-84	0.756	0.016	0.798	0.011	0.347	1.327
COB-4b-2-85	0.714	0.016	0.786	0.012	0.275	1.115
COB-4b-2-86	0.206	0.006	0.801	0.006	0.436	6.064
COB-4b-2-87	1.024	0.017	0.795	0.014	0.372	1.040
COB-4b-2-88	0.806	0.017	0.791	0.015	0.294	1.023
COB-4b-2-89	1.121	0.018	0.793	0.013	0.416	1.049
COB-4b-2-90	1.885	0.041	0.774	0.016	0.605	0.902
COB-4b-2-91	0.835	0.019	0.781	0.011	0.359	1.210
COB-4b-2-92	0.679	0.016	0.789	0.014	0.242	1.005
COB-4b-2-93	0.677	0.013	0.791	0.014	0.353	1.493
COB-4b-2-94	0.643	0.024	0.798	0.017	0.262	1.161
COB-4b-2-95	1.882	0.083	0.799	0.014	0.541	0.827
COB-4b-2-96	1.314	0.023	0.780	0.014	0.392	0.836
COB-4b-2-97	0.994	0.024	0.777	0.016	0.282	0.813
COB-4b-2-98	1.871	0.041	0.783	0.014	0.496	0.740
COB-4b-2-99	1.923	0.059	0.794	0.016	0.553	0.827
Palu-2						
Palu-2-1	53.49	5.67	0.674	0.046	1.820	0.101
Palu-2-2	194.08	13.61	0.355	0.031	2.343	0.016
Palu-2-3	115.45	7.83	0.444	0.029	2.338	0.035
Palu-2-4	178.71	13.79	0.339	0.030	1.574	0.013
Palu-2-5	197.32	14.08	0.277	0.023	2.874	0.012
Palu-2-6	239.33	21.49	0.151	0.029	1.467	0.003
Palu-2-7	255.50	17.77	0.103	0.014	3.132	0.003

Palu-2-8	235.08	32.41	0.222	0.087	0.365	0.001
Palu-2-9	210.09	20.44	0.211	0.030	1.849	0.006
Palu-2-10	301.86	29.30	0.122	0.026	1.436	0.002
Palu-2-11	208.73	15.21	0.215	0.021	2.124	0.007
Palu-2-12	286.33	22.11	0.100	0.016	3.736	0.003
Palu-2-13	138.79	9.94	0.455	0.032	1.756	0.022
Palu-2-14	196.48	16.45	0.338	0.050	1.414	0.007
Palu-2-15	237.40	18.80	0.159	0.023	1.731	0.004
Palu-2-16	246.97	18.46	0.145	0.017	2.438	0.004
Palu-2-17	251.37	19.73	0.127	0.018	2.047	0.003
Palu-2-18	153.95	18.06	0.373	0.047	1.460	0.017
Palu-2-19	214.08	17.49	0.217	0.023	1.624	0.006
Palu-2-20	196.06	14.85	0.294	0.025	2.138	0.011
Palu-2-21	145.60	13.12	0.443	0.048	1.712	0.019
Palu-2-22	158.53	11.80	0.422	0.035	1.827	0.017
Palu-2-23	230.62	18.04	0.192	0.018	2.612	0.007
Palu-2-24	153.18	12.26	0.446	0.034	1.621	0.018
Palu-2-25	137.91	12.27	0.430	0.030	1.691	0.022
Palu-2-26	151.51	11.09	0.442	0.037	1.229	0.014
Palu-2-27	68.56	5.09	0.599	0.025	2.941	0.111
Palu-2-28	64.22	4.82	0.592	0.022	2.934	0.122
Palu-2-29	98.63	7.56	0.565	0.025	2.608	0.066
Palu-2-30	145.45	10.42	0.449	0.030	1.549	0.020
Palu-2-31	122.02	9.86	0.552	0.039	1.660	0.032
Palu-2-32	205.32	17.61	0.362	0.040	1.838	0.015
Palu-2-33	167.56	14.12	0.481	0.045	1.460	0.016
Palu-2-34	276.59	23.58	0.128	0.023	1.905	0.002
Palu-2-35	231.73	16.18	0.193	0.024	2.879	0.006
Palu-2-36	161.88	14.55	0.408	0.035	1.722	0.018
Palu-2-37	157.77	12.71	0.486	0.038	1.580	0.019
Palu-2-38	179.47	17.81	0.379	0.037	1.103	0.008
Palu-2-39	189.40	15.95	0.312	0.032	1.681	0.010
Palu-2-40	193.42	14.98	0.346	0.028	2.204	0.014
Palu-2-41	175.31	12.01	0.348	0.030	1.471	0.010
Palu-2-42	215.52	18.47	0.240	0.024	1.624	0.006
Palu-2-43	186.88	14.57	0.361	0.030	1.790	0.012
Palu-2-44	220.56	16.15	0.224	0.022	2.007	0.006
Palu-2-45	265.07	19.24	0.126	0.014	3.193	0.004
Palu-2-46	286.66	18.69	0.080	0.007	7.108	0.003
Palu-2-47	212.31	15.63	0.245	0.021	2.559	0.010
Palu-2-48	115.84	9.12	0.455	0.025	2.619	0.039
Palu-2-49	161.77	12.52	0.362	0.031	2.047	0.017
Palu-2-50	172.68	12.98	0.356	0.027	1.942	0.015
Palu-2-51	150.00	12.12	0.425	0.033	2.628	0.030
Palu-2-52	158.17	11.99	0.394	0.029	2.363	0.024

Palu-2-53	172.70	11.19	0.332	0.022	2.419	0.016
Palu-2-54	177.78	13.72	0.307	0.025	2.905	0.017
Palu-2-55	151.71	11.65	0.390	0.027	1.944	0.020
Palu-2-56	142.52	10.41	0.424	0.035	1.457	0.014
Palu-2-57	257.13	22.89	0.154	0.024	1.594	0.002
Palu-2-58	190.41	14.60	0.289	0.034	2.319	0.013
Palu-2-59	236.50	16.86	0.148	0.013	4.042	0.006
Palu-2-60	244.93	22.78	0.205	0.033	1.881	0.005
Palu-2-61	245.14	19.06	0.119	0.018	2.679	0.003
Palu-2-62	235.60	18.03	0.172	0.020	2.132	0.005
Palu-2-63	207.11	16.12	0.234	0.026	1.695	0.008
Palu-2-64	222.84	19.13	0.252	0.025	2.663	0.010
Palu-2-65	219.32	21.20	0.251	0.033	2.286	0.009
Palu-2-66	271.08	19.19	0.099	0.015	3.304	0.002
Palu-2-67	257.13	17.78	0.114	0.011	5.491	0.006
Palu-2-68	248.88	19.77	0.191	0.019	3.037	0.005
Palu-2-69	177.42	13.13	0.339	0.025	2.604	0.018
Palu-2-70	196.10	14.61	0.280	0.029	1.821	0.009
Palu-2-71	258.53	22.35	0.142	0.025	2.064	0.003
Palu-2-72	247.36	17.36	0.183	0.018	2.926	0.007
Palu-2-73	252.80	17.21	0.135	0.013	4.597	0.005
Palu-2-74	214.61	16.95	0.263	0.032	2.230	0.009
Palu-2-75	267.11	20.89	0.118	0.017	2.473	0.003
Palu-2-76	128.24	8.42	0.431	0.024	3.017	0.041
Palu-2-77	76.46	5.19	0.581	0.027	2.653	0.085
Palu-2-78	3.02	0.21	0.843	0.010	8.068	9.162
Palu-2-79	1.92	0.13	0.838	0.010	8.219	14.510
Palu-2-80	0.59	0.12	0.793	0.098	0.004	0.020
Palu-2-81	255.75	8.79	0.105	0.015	3.938	0.004
Palu-2-82	256.25	21.89	0.115	0.017	2.731	0.003
Palu-2-83	254.26	18.10	0.138	0.016	3.792	0.006
Palu-2-84	212.43	15.65	0.260	0.029	2.017	0.008
Palu-2-85	235.92	17.23	0.108	0.018	2.320	0.002
Palu-2-86	215.42	16.48	0.178	0.019	2.195	0.006
Palu-2-87	263.33	19.48	0.110	0.013	3.794	0.002
Palu-3						
Palu-3-1	243.06	8.77	0.172	0.015	5.502	0.011
Palu-3-2	233.03	9.11	0.202	0.018	3.834	0.010
Palu-3-3	197.96	9.41	0.318	0.038	2.667	0.015
Palu-3-4	211.13	7.82	0.270	0.020	4.769	0.022
Palu-3-5	101.22	3.84	0.548	0.033	2.664	0.058
Palu-3-6	263.03	9.98	0.159	0.015	5.095	0.006
Palu-3-7	163.58	6.48	0.389	0.022	5.115	0.048
Palu-3-8	98.05	3.27	0.519	0.025	2.782	0.058
Palu-3-9	81.69	5.83	0.568	0.031	2.930	0.090

Palu-3-10	56.29	1.74	0.626	0.022	3.445	0.152
Palu-3-11	51.71	1.67	0.656	0.026	2.259	0.113
Palu-3-12	181.85	8.07	0.328	0.028	2.087	0.013
Palu-3-13	125.60	4.61	0.457	0.031	2.393	0.036
Palu-3-14	64.28	2.40	0.626	0.033	1.674	0.063
Palu-3-15	85.03	3.04	0.511	0.027	2.663	0.066
Palu-3-16	162.92	7.47	0.383	0.027	2.374	0.021
Palu-3-17	203.87	10.71	0.297	0.032	1.938	0.011
Palu-3-18	199.07	7.71	0.299	0.023	4.158	0.024
Palu-3-19	210.48	7.93	0.231	0.016	4.872	0.019
Palu-3-20	223.95	11.13	0.227	0.028	2.161	0.008
Palu-3-21	175.14	7.61	0.370	0.027	2.677	0.019
Palu-3-22	144.62	6.42	0.439	0.035	2.166	0.024
Palu-3-23	122.25	5.67	0.456	0.031	1.833	0.031
Palu-3-24	245.86	15.73	0.147	0.027	2.452	0.008
Palu-3-25	256.90	13.01	0.136	0.021	3.266	0.005
Palu-3-26	237.57	10.76	0.265	0.022	4.287	0.018
Palu-3-27	185.35	9.25	0.326	0.028	5.970	0.038
Palu-3-28	229.61	8.79	0.260	0.020	5.527	0.024
Palu-3-29	179.14	9.25	0.370	0.030	4.655	0.030
Palu-3-30	285.27	11.72	0.121	0.016	4.346	0.006
Palu-3-31	207.11	15.41	0.336	0.047	1.343	0.007
Palu-3-32	91.45	4.84	0.549	0.039	1.195	0.027
Palu-3-33	178.19	7.92	0.377	0.026	3.650	0.028
Palu-3-34	278.14	13.29	0.129	0.018	3.902	0.005
Palu-3-35	289.86	14.51	0.118	0.016	3.151	0.004
Palu-3-36	229.05	12.08	0.240	0.026	2.823	0.013
Palu-3-37	254.12	13.90	0.187	0.021	3.148	0.007
Palu-3-38	233.06	10.05	0.240	0.024	4.016	0.015
Palu-3-39	213.45	9.24	0.282	0.024	3.635	0.012
Palu-3-40	229.75	14.24	0.297	0.036	2.466	0.012
Palu-3-41	249.46	10.08	0.190	0.019	4.020	0.009
Palu-3-42	297.92	14.04	0.124	0.016	5.626	0.004
Palu-3-43	262.05	14.18	0.204	0.024	2.989	0.008
Palu-3-44	262.30	10.21	0.196	0.021	3.820	0.010
Palu-3-45	255.24	15.48	0.188	0.027	3.097	0.007
Palu-3-46	109.83	5.26	0.562	0.040	1.590	0.032
Palu-3-47	90.71	4.21	0.555	0.038	1.402	0.033
Palu-3-48	219.68	9.61	0.288	0.023	3.640	0.016
Palu-3-49	259.82	19.35	0.218	0.033	2.305	0.005
Palu-3-50	138.60	6.05	0.419	0.025	3.227	0.038
Palu-3-51	203.29	8.20	0.340	0.027	3.374	0.021
Palu-3-52	214.16	12.43	0.295	0.028	2.069	0.009
Palu-3-53	145.87	7.39	0.459	0.043	1.542	0.016
Palu-3-54	175.44	9.16	0.340	0.038	1.472	0.008

Palu-3-55	202.72	13.71	0.268	0.038	1.245	0.006
Palu-3-56	239.55	13.61	0.210	0.033	2.021	0.005
Palu-3-57	271.41	15.78	0.144	0.023	2.140	0.001
Palu-3-58	264.25	17.04	0.179	0.028	1.715	0.004
Palu-3-59	251.87	12.49	0.166	0.019	2.780	0.005
Palu-3-60	237.48	11.08	0.254	0.029	2.290	0.005
Palu-3-61	115.44	5.78	0.492	0.038	1.214	0.023
Palu-3-62	164.52	6.85	0.349	0.033	1.941	0.016
Palu-3-63	240.17	18.33	0.227	0.035	2.740	0.009
Palu-3-64	98.36	4.00	0.565	0.026	2.793	0.063
Palu-3-65	261.37	11.66	0.112	0.016	3.420	0.004
Palu-3-66	245.83	11.31	0.162	0.015	4.170	0.008
Palu-3-67	251.82	13.26	0.234	0.031	2.454	0.006
Palu-3-68	216.83	14.76	0.277	0.042	1.452	0.007
Palu-3-69	263.85	13.34	0.159	0.026	1.804	0.002
Palu-3-70	269.17	14.13	0.122	0.022	2.292	0.002
Palu-3-71	260.90	12.39	0.133	0.017	3.075	0.005
Palu-3-72	226.03	13.72	0.233	0.030	1.624	0.004
Palu-3-73	269.00	13.78	0.195	0.025	2.530	0.006
Palu-3-74	254.20	11.87	0.203	0.026	2.689	0.007
Palu-3-75	262.51	17.17	0.194	0.028	1.645	0.004
Palu-3-76	232.29	12.16	0.197	0.023	2.333	0.005
Palu-3-77	180.91	9.05	0.314	0.027	2.078	0.014
Palu-3-78	143.63	10.70	0.427	0.048	1.036	0.011
Palu-3-79	211.02	9.09	0.277	0.024	1.893	0.011
Palu-3-80	149.97	6.61	0.398	0.030	1.936	0.019
Palu-3-81	136.14	7.21	0.458	0.040	1.391	0.018
Palu-3-82	262.52	13.78	0.148	0.022	2.229	0.004
Palu-3-83	24.67	0.85	0.735	0.020	1.478	0.189
Palu-3-84	96.61	4.87	0.596	0.031	2.545	0.063
Palu-3-85	104.16	4.73	0.486	0.032	1.304	0.025
Palu-3-86	132.43	5.90	0.426	0.030	2.090	0.029
Palu-3-87	123.60	6.13	0.459	0.036	1.820	0.029
Palu-4						
Palu-4-1	233.67	11.43	0.200	0.020	3.707	0.012
Palu-4-2	248.33	12.04	0.175	0.019	2.788	0.007
Palu-4-3	90.53	5.49	0.621	0.036	2.502	0.070
Palu-4-4	198.74	15.34	0.312	0.032	3.981	0.032
Palu-4-5	215.58	10.39	0.237	0.029	3.718	0.017
Palu-4-6	79.61	6.20	0.626	0.031	3.409	0.125
Palu-4-7	66.79	6.36	0.634	0.030	2.067	0.103
Palu-4-8	254.09	9.92	0.141	0.015	4.212	0.007
Palu-4-9	39.86	2.41	0.697	0.020	2.141	0.155
Palu-4-10	26.56	1.35	0.706	0.013	3.723	0.416
Palu-4-11	49.28	2.80	0.658	0.018	2.863	0.160

Palu-4-12	59.82	2.82	0.637	0.022	2.861	0.126
Palu-4-13	98.46	5.38	0.533	0.024	3.479	0.076
Palu-4-14	121.40	6.43	0.481	0.029	2.329	0.040
Palu-4-15	45.65	2.03	0.676	0.021	2.742	0.168
Palu-4-16	72.16	5.10	0.635	0.028	2.522	0.096
Palu-4-17	227.88	14.67	0.240	0.029	3.017	0.011
Palu-4-18	246.18	12.07	0.178	0.022	2.069	0.004
Palu-4-19	263.37	16.42	0.190	0.034	1.618	0.004
Palu-4-20	278.74	15.24	0.111	0.016	2.777	0.003
Palu-4-21	273.03	13.00	0.109	0.014	2.457	0.003
Palu-4-22	95.57	6.09	0.602	0.027	2.347	0.060
Palu-4-23	108.29	8.24	0.591	0.035	3.063	0.073
Palu-4-24	138.10	11.55	0.516	0.036	1.866	0.034
Palu-4-25	239.94	15.05	0.271	0.032	2.308	0.010
Palu-4-26	150.60	6.50	0.446	0.030	2.637	0.029
Palu-4-27	145.09	9.75	0.445	0.032	2.097	0.025
Palu-4-28	192.07	12.36	0.336	0.028	2.530	0.016
Palu-4-29	143.57	12.22	0.427	0.039	4.561	0.060
Palu-4-30	154.79	11.17	0.407	0.031	5.933	0.072
Palu-4-31	172.95	10.02	0.367	0.032	4.105	0.035
Palu-4-32	213.35	14.96	0.271	0.033	5.170	0.030
Palu-4-33	169.55	12.48	0.376	0.040	2.156	0.021
Palu-4-34	238.06	13.25	0.206	0.021	2.574	0.009
Palu-4-35	251.34	12.57	0.158	0.019	2.754	0.005
Palu-4-36	235.23	13.12	0.195	0.024	2.886	0.005
Palu-4-37	227.97	12.17	0.174	0.027	2.211	0.006
Palu-4-38	245.06	11.80	0.198	0.020	2.251	0.005
Palu-4-39	208.17	12.66	0.286	0.034	2.571	0.014
Palu-4-40	174.29	10.83	0.392	0.029	2.005	0.018
Palu-4-41	61.48	6.25	0.633	0.021	3.579	0.187
Palu-4-42	176.52	9.35	0.338	0.024	6.714	0.055
Palu-4-43	90.60	8.09	0.560	0.034	2.190	0.061
Palu-4-44	260.47	14.44	0.129	0.020	2.292	0.003
Palu-4-45	245.43	15.64	0.253	0.031	2.217	0.009
Palu-4-46	283.46	13.75	0.071	0.010	5.157	0.001
Palu-4-47	206.11	14.48	0.254	0.033	3.188	0.018
Palu-4-48	249.45	16.14	0.220	0.040	1.919	0.004
Palu-4-49	288.59	16.30	0.128	0.017	3.970	0.005
Palu-4-50	157.62	9.24	0.423	0.039	2.301	0.026
Palu-4-51	82.00	5.27	0.604	0.029	2.604	0.077
Palu-4-52	260.21	15.09	0.226	0.026	2.572	0.007
Palu-4-53	235.90	12.76	0.221	0.028	4.694	0.019
Palu-4-54	252.21	11.01	0.183	0.017	3.751	0.009
Palu-4-55	161.06	15.87	0.427	0.040	4.054	0.048
Palu-4-56	234.07	13.79	0.220	0.024	2.871	0.007

Palu-4-57	242.76	13.79	0.219	0.020	3.290	0.012
Palu-4-58	253.02	13.72	0.147	0.023	3.877	0.007
Palu-4-59	258.61	13.37	0.161	0.020	4.732	0.008
Palu-4-60	259.89	15.33	0.194	0.025	2.252	0.005
Palu-4-61	293.10	17.68	0.123	0.017	3.217	0.005
Palu-4-62	282.89	13.85	0.138	0.018	2.901	0.004
Palu-4-63	178.49	12.99	0.344	0.031	2.548	0.022
Palu-4-64	171.50	14.01	0.405	0.040	3.098	0.039
Palu-4-65	102.13	9.12	0.525	0.037	2.241	0.052
Palu-4-66	239.94	13.61	0.182	0.019	2.558	0.007
Palu-4-67	222.39	13.22	0.270	0.028	1.863	0.008
Palu-4-68	178.58	8.48	0.333	0.025	1.922	0.013
Palu-4-69	102.00	6.43	0.511	0.034	2.006	0.039
Palu-4-70	211.67	12.19	0.244	0.026	2.448	0.009
Palu-4-71	117.91	10.08	0.538	0.029	3.358	0.076
Palu-4-72	74.44	3.85	0.617	0.029	2.682	0.091
Palu-4-73	273.21	14.82	0.128	0.021	2.771	0.003
Palu-4-74	165.43	8.21	0.376	0.028	2.831	0.027
Palu-4-75	208.64	16.17	0.256	0.028	3.628	0.015
Palu-4-76	189.21	14.15	0.335	0.026	3.930	0.029
Palu-4-77	79.13	5.99	0.570	0.025	2.394	0.077
Palu-4-78	62.90	4.88	0.607	0.017	2.818	0.117
Palu-4-79	41.82	3.07	0.673	0.022	2.882	0.188
Palu-4-80	45.28	3.60	0.674	0.026	2.260	0.142
Palu-4-81	70.13	4.87	0.561	0.026	1.793	0.062
Palu-4-82	259.18	20.05	0.151	0.014	2.605	0.006
Palu-4-83	254.61	17.76	0.139	0.015	3.055	0.005
Palu-4-84	212.27	15.38	0.260	0.020	2.776	0.013
Palu-4-85	259.81	18.15	0.113	0.014	3.166	0.004
Palu-4-86	222.94	16.30	0.249	0.022	3.055	0.013
Palu-4-87	250.06	18.55	0.151	0.017	2.612	0.005
Palu-4-88	201.43	14.52	0.300	0.043	1.310	0.007
Palu-4-89	266.76	18.02	0.139	0.013	3.728	0.006
Palu-4-90	245.57	15.90	0.164	0.018	3.415	0.010
Palu-4-91	255.92	18.34	0.156	0.017	2.943	0.006
Palu-4-92	262.00	18.55	0.117	0.013	3.942	0.006
Palu-4-93	250.50	19.69	0.153	0.019	2.920	0.005
Palu-4-94	259.67	18.16	0.132	0.016	5.885	0.010
Palu-4-95	265.57	18.89	0.137	0.014	4.262	0.006
Palu-4-96	245.06	20.96	0.134	0.020	2.614	0.007
Palu-4-97	155.28	18.72	0.408	0.057	2.815	0.041
TRK- 4						
TRK-4-1	17.943	0.619	0.717	0.020	0.316	0.049
TRK-4-2	44.389	1.356	0.626	0.028	0.355	0.018
TRK-4-3	42.244	1.542	0.699	0.033	0.250	0.015

TRK-4-4	48.491	1.649	0.645	0.026	0.494	0.027
TRK-4-5	20.437	1.038	0.732	0.023	0.358	0.054
TRK-4-6	55.551	1.202	0.637	0.016	1.901	0.090
TRK-4-7	62.493	2.012	0.608	0.019	1.277	0.049
TRK-4-8	83.474	3.076	0.587	0.023	1.274	0.037
TRK-4-9	70.382	2.414	0.604	0.032	0.568	0.018
TRK-4-10	34.897	1.454	0.717	0.039	0.203	0.016
TRK-4-11	100.246	2.924	0.544	0.017	2.652	0.057
TRK-4-12	72.029	4.435	0.582	0.022	1.117	0.040
TRK-4-13	46.186	3.046	0.608	0.046	0.803	0.040
TRK-4-14	91.449	4.811	0.495	0.045	0.852	0.018
TRK-4-15	80.009	1.968	0.600	0.020	2.323	0.070
TRK-4-16	105.373	3.073	0.492	0.022	1.258	0.021
TRK-4-17	47.471	2.708	0.652	0.034	0.315	0.018
TRK-4-18	18.253	0.820	0.740	0.039	0.088	0.014
TRK-4-19	92.165	2.610	0.561	0.022	1.453	0.034
TRK-4-20	73.232	4.137	0.544	0.025	0.537	0.017
TRK-4-21	79.612	2.698	0.550	0.030	0.485	0.012
TRK-4-22	81.369	3.255	0.537	0.026	0.687	0.018
TRK-4-23	89.866	2.369	0.517	0.019	1.301	0.028
TRK-4-24	101.329	3.546	0.491	0.027	0.687	0.012
TRK-4-25	62.283	5.008	0.563	0.038	0.484	0.017
TRK-4-26	60.666	3.374	0.575	0.039	0.526	0.016
TRK-4-27	104.778	3.301	0.508	0.023	0.929	0.017
TRK-4-28	51.417	5.360	0.611	0.052	0.395	0.019
TRK-4-29	110.205	2.968	0.494	0.020	1.634	0.028
TRK-4-30	82.849	3.859	0.527	0.025	0.730	0.020
TRK-4-31	86.288	3.916	0.552	0.024	1.269	0.032
TRK-4-32	55.141	4.566	0.614	0.032	0.438	0.019
TRK-4-33	92.624	2.619	0.536	0.023	1.729	0.040
TRK-4-34	53.691	2.408	0.615	0.031	0.328	0.015
TRK-4-35	51.124	3.821	0.664	0.037	0.391	0.021
TRK-4-36	22.880	2.014	0.699	0.032	0.226	0.033
TRK-4-37	4.285	0.227	0.790	0.043	0.026	0.019
TRK-4-38	3.721	0.386	0.777	0.039	0.037	0.050
TRK-4-39	6.812	0.639	0.810	0.101	0.015	0.007
TRK-4-40	37.907	4.807	0.707	0.092	0.072	0.005
TRK-4-41	25.342	1.303	0.712	0.035	0.148	0.016
TRK-4-42	4.049	0.215	0.778	0.032	0.038	0.030
TRK-4-43	2.055	0.196	0.872	0.102	0.005	0.007
TRK-4-44	2.327	0.114	0.779	0.049	0.008	0.010
TRK-4-45	1.807	0.164	0.785	0.077	0.003	0.005
TRK-4-46	0.516	0.026	0.765	0.027	0.004	0.024
TRK-4-47	2.257	0.096	0.765	0.041	0.011	0.015
TRK-4-48	0.352	0.014	0.796	0.017	0.024	0.222

TRK-4-49	1.812	0.141	0.751	0.044	0.006	0.012
TRK-4-50	1.514	0.078	0.815	0.038	0.008	0.017
TRK-4-51	0.637	0.036	0.757	0.034	0.004	0.020
TRK-4-52	0.060	0.002	0.782	0.008	0.037	1.968
TRK-4-53	32.786	1.883	0.739	0.052	0.093	0.008
TRK-4-54	1.515	0.250	0.801	0.040	0.008	0.018
TRK-4-55	0.934	0.053	0.818	0.046	0.004	0.013
TRK-4-56	0.243	0.013	0.799	0.021	0.012	0.176
TRK-4-57	25.390	1.738	0.759	0.039	0.139	0.015
TRK-4-58	6.602	2.044	0.766	0.142	0.024	0.013
TRK-4-59	0.702	0.051	0.781	0.061	0.006	0.024
TRK-4-60	0.651	0.022	0.771	0.013	0.036	0.176
TRK-4-61	19.295	1.031	0.668	0.042	0.131	0.017
TRK-4-62	14.237	0.918	0.751	0.063	0.076	0.017
TRK-4-63	67.682	2.705	0.528	0.022	1.300	0.040
TRK-4-64	2.441	0.129	0.830	0.044	0.012	0.015
TRK-4-65	8.079	0.483	0.757	0.057	0.019	0.007
TRK-4-66	13.519	0.815	0.744	0.061	0.030	0.006
TRK-4-67	2.150	0.092	0.792	0.033	0.021	0.032
TRK-4-68	5.686	0.616	0.735	0.023	0.104	0.061
TRK-4-69	4.434	0.208	0.735	0.042	0.029	0.019
TRK-4-70	0.878	0.078	0.813	0.060	0.002	0.006
TRK-4-71	1.248	0.078	0.839	0.056	0.004	0.012
TRK-4-72	32.000	2.284	0.710	0.044	0.127	0.010
TRK-4-73	1.791	0.133	0.767	0.060	0.003	0.006
TRK-4-74	1.824	0.315	0.853	0.145	0.002	0.002
TRK-4-75	4.202	0.305	0.812	0.040	0.034	0.026
TRK-4-76	2.782	0.373	0.849	0.083	0.012	0.016
TRK-4-77	32.113	2.091	0.648	0.050	0.078	0.007
TRK-4-78	17.586	0.876	0.776	0.041	0.150	0.026
TRK-4-79	18.567	0.892	0.702	0.033	0.155	0.025
TRK-4-80	1.121	0.060	0.816	0.028	0.017	0.049
TRK-4-81	1.763	0.200	0.773	0.070	0.002	0.005
TRK-4-82	0.451	0.076	0.847	0.105	0.001	0.009
TRK-4-83	12.049	0.586	0.774	0.033	0.215	0.055
TRK-4-84	32.785	1.559	0.702	0.032	0.337	0.028
TRK-4-85	71.200	3.525	0.600	0.026	0.733	0.025
TRK-4-86	5.123	0.360	0.766	0.053	0.014	0.008
TRK-4-87	1.689	0.098	0.777	0.044	0.009	0.016
TRK-4-88	3.419	0.211	0.765	0.037	0.021	0.018
TRK-4-89	4.696	0.857	0.797	0.131	0.007	0.003
TRK-4-90	27.705	1.818	0.670	0.047	0.128	0.012
TRK-4-91	11.554	0.760	0.783	0.036	0.084	0.022
TRK-4-92	35.854	1.999	0.672	0.058	0.077	0.006
TRK-4-93	30.357	1.939	0.696	0.041	0.172	0.017

TRK-4-94	99.827	5.910	0.543	0.044	0.507	0.011
TRK-4-95	9.105	0.684	0.746	0.073	0.018	0.006
TRK-4-96	2.838	0.383	0.800	0.116	0.002	0.003
TRK-4-97	101.448	5.502	0.564	0.026	1.657	0.035
TRK-4-98	63.946	4.731	0.600	0.026	1.338	0.061
TRK-1a						
TRK-1a-1	54.784	3.524	0.676	0.066	0.401	0.021
TRK-1a-2	13.029	0.778	0.741	0.061	0.097	0.021
TRK-1a-3	32.475	1.151	0.667	0.027	0.641	0.055
TRK-1a-4	34.858	2.042	0.663	0.034	0.456	0.034
TRK-1a-5	34.032	1.643	0.687	0.053	0.218	0.018
TRK-1a-6	18.450	1.188	0.754	0.052	0.248	0.040
TRK-1a-7	43.974	3.079	0.614	0.060	0.286	0.016
TRK-1a-8	23.307	1.481	0.745	0.047	0.167	0.024
TRK-1a-9	33.912	3.065	0.719	0.118	0.176	0.014
TRK-1a-10	38.308	2.923	0.676	0.064	0.188	0.014
TRK-1a-11	22.888	1.610	0.683	0.039	0.197	0.027
TRK-1a-12	6.998	0.419	0.734	0.046	0.056	0.025
TRK-1a-13	17.912	1.086	0.700	0.038	0.177	0.029
TRK-1a-14	28.330	2.231	0.733	0.065	0.124	0.011
TRK-1a-15	30.253	1.503	0.681	0.053	0.248	0.022
TRK-1a-16	41.044	1.342	0.647	0.031	0.498	0.030
TRK-1a-17	25.363	0.475	0.706	0.015	1.734	0.190
TRK-1a-18	37.321	0.875	0.626	0.025	0.887	0.058
TRK-1a-19	24.597	1.718	0.659	0.038	0.227	0.025
TRK-1a-20	19.059	1.947	0.696	0.042	0.210	0.065
TRK-1a-21	25.279	1.011	0.690	0.031	0.418	0.044
TRK-1a-22	29.116	0.591	0.655	0.020	1.066	0.096
TRK-1a-23	33.933	0.804	0.657	0.023	0.907	0.068
TRK-1a-24	34.619	0.712	0.656	0.018	1.557	0.116
TRK-1a-25	27.806	1.040	0.679	0.040	0.296	0.027
TRK-1a-26	29.662	2.213	0.700	0.051	0.195	0.021
TRK-1a-27	22.192	1.643	0.675	0.064	0.156	0.020
TRK-1a-28	25.177	0.918	0.676	0.030	0.367	0.038
TRK-1a-29	25.607	0.568	0.695	0.018	1.259	0.131
TRK-1a-30	30.417	0.789	0.701	0.024	0.932	0.082
TRK-1a-31	33.395	0.795	0.660	0.020	1.036	0.081
TRK-1a-32	29.257	0.706	0.665	0.018	0.889	0.079
TRK-1a-33	34.904	2.062	0.695	0.045	0.286	0.021
TRK-1a-34	25.096	3.518	0.648	0.130	0.070	0.007
TRK-1a-35	29.009	0.882	0.673	0.028	0.543	0.048
TRK-1a-36	25.175	0.416	0.689	0.017	1.571	0.174
TRK-1a-37	25.972	0.406	0.694	0.014	1.902	0.204
TRK-1a-38	30.217	0.806	0.641	0.024	0.863	0.073
TRK-1a-39	20.906	1.575	0.737	0.051	0.183	0.027

TRK-1a-40	19.367	1.235	0.748	0.046	0.156	0.025
TRK-1a-41	30.386	0.801	0.670	0.022	0.895	0.076
TRK-1a-42	26.506	0.489	0.703	0.016	1.862	0.197
TRK-1a-43	27.018	0.480	0.685	0.017	1.728	0.180
TRK-1a-44	26.227	1.278	0.645	0.026	0.815	0.083
TRK-1a-45	34.812	1.225	0.625	0.030	0.502	0.038
TRK-1a-46	31.051	1.930	0.694	0.051	0.172	0.015
TRK-1a-47	33.750	2.652	0.653	0.032	0.668	0.064
TRK-1a-48	28.968	1.571	0.658	0.026	0.527	0.050
TRK-1a-49	25.705	1.219	0.664	0.028	0.347	0.037
TRK-1a-50	28.585	0.808	0.680	0.025	0.660	0.065
TRK-1a-51	25.883	0.529	0.679	0.018	1.109	0.118
TRK-1a-52	32.634	0.955	0.654	0.022	0.878	0.072
TRK-1a-53	37.204	1.375	0.705	0.026	0.862	0.066
TRK-1a-54	28.680	0.897	0.699	0.032	0.414	0.039
TRK-1a-55	37.534	2.866	0.656	0.053	0.181	0.015
TRK-1a-56	27.455	0.660	0.672	0.021	0.947	0.092
TRK-1a-57	19.847	0.422	0.655	0.020	0.811	0.107
TRK-1a-58	36.535	1.284	0.661	0.026	0.802	0.059
TRK-1a-59	32.229	1.248	0.675	0.043	0.296	0.026
TRK-1a-60	32.360	1.623	0.713	0.041	0.371	0.035
TRK-1a-61	27.929	1.685	0.677	0.040	0.248	0.025
TRK-1a-62	25.435	0.742	0.691	0.024	0.761	0.083
TRK-1a-63	22.244	0.572	0.665	0.018	0.897	0.113
TRK-1a-64	53.931	2.593	0.616	0.038	0.643	0.026
TRK-1a-65	26.218	1.329	0.719	0.042	0.217	0.024
TRK-1a-66	26.132	1.430	0.670	0.053	0.189	0.019
TRK-1a-67	27.032	0.985	0.724	0.035	0.401	0.040
TRK-1a-68	22.615	0.585	0.690	0.017	0.967	0.111
TRK-1a-69	31.156	2.118	0.696	0.033	0.520	0.055
TRK-1a-70	20.723	1.285	0.727	0.059	0.118	0.018
TRK-1a-71	23.886	2.361	0.653	0.075	0.204	0.020
TRK-1a-72	27.887	0.915	0.636	0.030	0.527	0.047
TRK-1a-73	25.071	2.074	0.669	0.037	0.285	0.037
TRK-1a-74	31.696	1.352	0.676	0.023	1.083	0.090
TRK-1a-75	41.954	3.116	0.670	0.063	0.490	0.029
TRK-1a-76	25.962	0.656	0.640	0.027	0.626	0.060
TRK-1a-77	31.018	0.648	0.664	0.019	1.167	0.099
TRK-1a-78	26.125	0.889	0.645	0.028	0.487	0.047
TRK-1a-79	34.111	1.295	0.626	0.026	0.636	0.045
TRK-1a-80	37.809	2.465	0.659	0.046	0.363	0.028
TRK-1a-81	62.500	2.302	0.586	0.033	0.721	0.026
TRK-1a-82	28.143	0.773	0.654	0.020	1.053	0.092
TRK-1a-83	32.287	0.807	0.625	0.023	1.043	0.081
TRK-1a-84	24.633	0.866	0.644	0.026	0.506	0.052

TRK-1a-85	30.582	1.216	0.697	0.028	0.850	0.084
TRK-1a-86	36.828	2.268	0.698	0.039	0.390	0.031
TRK-1a-87	32.229	0.841	0.626	0.025	0.738	0.057
TRK-1a-88	41.152	2.112	0.608	0.028	0.609	0.036
TRK-1a-89	31.147	0.843	0.675	0.021	1.179	0.104
TRK-1a-90	32.267	1.106	0.642	0.028	0.571	0.047
TRK-1a-91	52.130	2.713	0.624	0.048	0.354	0.018
TRK-1a-92	56.879	2.235	0.644	0.032	0.853	0.036
TRK-1a-93	34.000	0.935	0.643	0.019	1.071	0.083
TRK-1a-94	26.514	0.486	0.684	0.016	1.577	0.165
TRK-1a-95	42.939	1.414	0.630	0.033	0.624	0.037
TRK-1a-96	37.544	1.492	0.631	0.027	0.762	0.050
TRK-1a-97	26.838	0.442	0.675	0.016	1.329	0.137
TRK-1a-98	25.452	0.832	0.645	0.023	0.653	0.070
TRK-1a-99	32.157	0.875	0.653	0.026	0.689	0.055
HRM-1						
HRM-1-1	57.247	12.697	0.786	0.210	0.036	0.001
HRM-1-2	40.537	16.709	0.833	0.184	0.023	0.004
HRM-1-3	21.692	8.705	0.802	0.247	0.009	0.001
HRM-1-4	13.015	10.715	0.751	0.291	0.006	0.001
HRM-1-5	10.772	2.753	0.970	0.244	0.009	0.003
HRM-1-6	6.831	0.485	0.746	0.048	0.071	0.035
HRM-1-7	83.526	27.965	0.956	0.341	0.066	0.003
HRM-1-8	5.949	0.391	0.760	0.042	0.053	0.030
HRM-1-9	58.857	19.777	0.853	0.372	0.040	0.003
HRM-1-10	39.432	17.087	0.669	0.252	0.032	0.002
HRM-1-11	66.516	4.803	0.677	0.046	0.241	0.010
HRM-1-12	31.950	2.149	0.721	0.043	0.125	0.013
HRM-1-13	8.216	0.501	0.753	0.052	0.031	0.012
HRM-1-14	17.600	1.258	0.790	0.047	0.108	0.019
HRM-1-15	66.747	14.529	0.825	0.198	0.036	0.002
HRM-1-16	79.290	24.003	0.701	0.184	0.041	0.001
HRM-1-17	4.975	0.435	0.766	0.019	0.226	0.159
HRM-1-18	9.597	0.452	0.758	0.038	0.070	0.022
HRM-1-19	96.335	9.922	0.733	0.097	0.146	0.005
HRM-1-20	127.993	57.592	0.760	0.228	0.059	0.001
HRM-1-21	151.764	26.102	0.839	0.240	0.187	0.002
HRM-1-22	14.096	0.796	0.811	0.056	0.049	0.011
HRM-1-23	105.562	103.066	0.594	0.858	0.023	0.000
HRM-1-24	157.854	50.040	0.805	0.498	0.025	0.000
HRM-1-25	21.813	2.317	0.823	0.076	0.040	0.007
HRM-1-26	59.016	22.951	0.736	0.433	0.024	0.001
HRM-1-27	31.502	10.273	0.576	0.145	0.032	0.002
HRM-1-28	28.790	8.303	0.855	0.327	0.021	0.003
HRM-1-29	78.532	22.086	0.744	0.195	0.049	0.002

HRM-1-30	38.030	17.610	0.758	0.119	0.037	0.009
HRM-1-31	80.509	36.219	0.716	0.288	0.052	0.003
HRM-1-32	144.859	71.012	0.636	0.353	0.051	0.001
HRM-1-33	27.849	8.789	0.832	0.225	0.057	0.008
HRM-1-34	156.152	210.621	0.539	0.384	0.032	0.001
HRM-1-35	108.679	57.288	0.946	0.460	0.041	0.001
HRM-1-36	205.777	177.330	0.510	0.663	0.036	0.000
HRM-1-37	147.074	102.600	0.570	0.280	0.056	0.001
HRM-1-38	67.424	12.864	0.510	0.197	0.079	0.003
HRM-1-39	72.137	9.288	0.797	0.086	0.067	0.004
HRM-1-40	74.779	4.556	0.727	0.066	0.150	0.006
HRM-1-41	92.973	9.712	0.797	0.094	0.100	0.003
HRM-1-42	128.233	140.943	0.455	0.483	0.081	0.000
HRM-1-43	380.937	127.196	0.540	0.326	0.109	0.000
HRM-1-44	142.934	21.619	0.832	0.146	0.075	0.001
HRM-1-45	100.020	11.619	0.791	0.119	0.086	0.003
HRM-1-46	229.882	53.911	0.721	0.230	0.135	0.002
HRM-1-47	72.592	9.276	0.850	0.105	0.108	0.005
HRM-1-48	174.526	25.030	0.748	0.097	0.220	0.004
HRM-1-49	174.074	34.421	0.912	0.182	0.115	0.002
HRM-1-50	25.134	1.953	0.737	0.060	0.060	0.008
HRM-1-51	25.123	1.432	0.740	0.035	0.156	0.020
HRM-1-52	10.510	0.729	0.830	0.067	0.025	0.007
HRM-1-53	82.191	26.341	0.971	0.269	0.057	0.004
HRM-1-54	29.826	15.297	0.595	0.269	0.023	0.003
HRM-1-55	132.089	54.284	0.754	0.217	0.070	0.004
HRM-1-56	47.796	6.141	0.801	0.100	0.062	0.004
HRM-1-57	30.498	1.511	0.743	0.048	0.113	0.012
HRM-1-58	21.288	0.718	0.738	0.015	1.194	0.184
HRM-1-59	185.620	51.890	0.786	0.245	0.099	0.002
HRM-1-60	22.839	1.847	0.851	0.071	0.051	0.008
HRM-1-61	17.649	0.712	0.746	0.034	0.150	0.027
HRM-1-62	7.244	0.751	0.983	0.114	0.008	0.005
HRM-1-63	18.694	2.378	0.934	0.102	0.028	0.006
HRM-1-64	10.186	0.668	0.784	0.040	0.105	0.033
HRM-1-65	16.642	2.527	1.107	0.155	0.015	0.005
HRM-1-66	29.228	4.041	0.806	0.044	0.178	0.046
HRM-1-67	3.649	0.185	0.804	0.047	0.023	0.020
HRM-1-68	8.562	0.295	0.754	0.023	0.226	0.086
HRM-1-69	23.356	0.826	0.735	0.022	0.409	0.056
HRM-1-70	74.454	10.321	0.737	0.098	0.099	0.005
HRM-1-71	154.309	15.228	0.676	0.094	0.124	0.002
HRM-1-72	28.856	0.869	0.726	0.012	2.439	0.263
HRM-1-73	22.978	1.175	0.733	0.015	1.585	0.228
HRM-1-74	11.083	0.981	0.760	0.017	1.259	0.446

HRM-1-75	37.587	6.267	0.765	0.051	0.141	0.056
HRM-1-76	89.996	8.853	0.773	0.076	0.175	0.007
HRM-1-77	15.519	0.940	0.689	0.024	0.406	0.091
HRM-1-78	39.133	3.518	0.703	0.033	0.378	0.044
HRM-1-79	9.356	0.701	0.760	0.023	3.807	1.421
HRM-1-80	93.019	11.223	0.843	0.161	0.058	0.002
HRM-1-81	34.079	1.515	0.746	0.018	1.367	0.123
HRM-1-82	108.261	24.410	0.866	0.323	0.050	0.001
HRM-1-83	11.950	0.448	0.749	0.017	0.367	0.102
HRM-1-84	30.061	1.264	0.765	0.024	0.379	0.040
HRM-1-85	14.233	1.332	0.757	0.017	3.259	1.054
HRM-1-86	8.403	1.182	0.825	0.075	0.017	0.008
HRM-1-87	14.265	1.157	0.746	0.025	0.152	0.035
HRM-1-88	11.874	0.737	0.753	0.017	0.470	0.132
HRM-1-89	19.868	3.131	0.764	0.043	3.647	1.314
HRM-1-90	25.630	1.394	0.744	0.016	3.023	0.379
HRM-1-91	24.574	2.815	0.741	0.018	2.328	0.451
HRM-1-92	207.056	20.138	0.676	0.067	0.295	0.005
HRM-1-93	125.251	7.028	0.706	0.059	0.280	0.006
HRM-1-94	44.421	2.960	0.805	0.073	0.091	0.008
HRM-1-95	52.405	4.081	0.799	0.078	0.088	0.006
HRM-1-96	91.042	10.171	0.865	0.127	0.095	0.003
HRM-1-97	32.672	2.121	0.767	0.052	0.081	0.007
HRM-1-98	83.097	67.375	0.528	0.486	0.029	0.000
HRM-2						
HRM-2-1	65.662	3.368	0.713	0.051	0.207	0.010
HRM-2-2	458.728	55.867	0.332	0.076	0.683	0.002
HRM-2-3	26.855	5.632	0.764	0.236	0.011	0.001
HRM-2-4	37.455	2.161	0.789	0.082	0.075	0.006
HRM-2-5	140.723	8.967	0.695	0.054	0.358	0.007
HRM-2-6	8.561	0.246	0.756	0.013	0.766	0.291
HRM-2-7	230.405	93.496	0.554	0.507	0.059	0.000
HRM-2-8	325.688	25.348	0.525	0.065	0.400	0.002
HRM-2-9	7.340	1.395	0.905	0.183	0.005	0.003
HRM-2-10	267.733	24.033	0.611	0.072	0.332	0.004
HRM-2-11	88.062	18.828	0.861	0.236	0.072	0.003
HRM-2-12	166.992	11.786	0.601	0.066	0.221	0.003
HRM-2-13	131.211	40.002	0.708	0.221	0.073	0.001
HRM-2-14	402.052	94.920	0.438	0.108	0.215	0.001
HRM-2-15	3.018	1.309	0.803	0.299	0.004	0.011
HRM-2-16	162.447	17.489	0.669	0.088	0.100	0.002
HRM-2-17	70.885	4.039	0.674	0.052	0.284	0.012
HRM-2-18	182.367	43.923	0.546	0.159	0.102	0.002
HRM-2-19	328.016	155.108	0.456	0.545	0.046	0.000
HRM-2-20	49.341	27.007	0.457	0.627	0.005	0.000

HRM-2-21	21.927	9.591	0.590	0.225	0.013	0.002
HRM-2-22	123.017	27.017	0.564	0.255	0.055	0.002
HRM-2-23	177.942	63.437	0.426	0.414	0.050	0.000
HRM-2-24	404.597	157.638	0.567	0.277	0.077	0.000
HRM-2-25	149.638	61.125	0.585	0.414	0.074	0.001
HRM-2-26	345.940	78.732	0.602	0.171	0.115	0.001
HRM-2-27	25.822	1.752	0.841	0.058	0.075	0.009
HRM-2-28	139.973	46.499	0.703	0.232	0.064	0.006
HRM-2-29	118.306	58.463	0.494	0.445	0.051	0.001
HRM-2-30	157.125	52.822	0.499	0.296	0.059	0.001
HRM-2-31	126.279	92.468	0.639	0.414	0.063	0.003
HRM-2-32	319.260	72.024	0.426	0.305	0.163	0.001
HRM-2-33	76.629	12.054	0.817	0.137	0.120	0.007
HRM-2-34	36.607	4.603	0.801	0.155	0.056	0.006
HRM-2-35	346.317	72.015	0.645	0.181	0.221	0.001
HRM-2-36	282.043	46.849	0.457	0.268	0.112	0.000
HRM-2-37	519.921	71.226	0.337	0.095	0.330	0.001
HRM-2-38	260.374	29.548	0.542	0.095	0.201	0.002
HRM-2-39	323.893	20.669	0.495	0.058	0.480	0.003
HRM-2-40	257.425	61.634	0.816	0.322	0.080	0.001
HRM-2-41	286.277	97.059	0.775	0.368	0.093	0.001
HRM-2-42	326.982	53.527	0.456	0.116	0.371	0.003
HRM-2-43	196.176	13.981	0.617	0.062	0.324	0.004
HRM-2-44	42.625	3.170	0.764	0.084	0.065	0.005
HRM-2-45	30.915	1.158	0.743	0.027	0.553	0.059
HRM-2-46	46.437	2.607	0.722	0.031	0.554	0.038
HRM-2-47	14.635	0.441	0.779	0.023	0.291	0.063
HRM-2-48	5.002	0.636	0.793	0.029	0.092	0.104
HRM-2-49	238.120	15.114	0.543	0.053	0.498	0.005
HRM-2-50	35.587	1.217	0.694	0.018	2.851	0.240
HRM-2-51	20.987	1.884	0.742	0.015	1.488	0.368
HRM-2-52	579.762	56.641	0.242	0.059	0.445	0.000
HRM-2-53	137.762	9.935	0.647	0.057	0.269	0.006
HRM-2-54	63.450	2.402	0.695	0.034	0.414	0.018
HRM-2-55	36.191	0.666	0.693	0.010	3.412	0.274
HRM-2-56	69.965	6.026	0.712	0.038	0.481	0.031
HRM-2-57	233.800	15.301	0.611	0.061	0.448	0.005
HRM-2-58	535.653	31.285	0.340	0.044	0.741	0.001
HRM-2-59	566.920	40.159	0.224	0.042	0.744	0.001
HRM-2-60	18.214	2.236	0.735	0.015	1.039	0.249
HRM-2-61	22.672	1.190	0.718	0.014	1.726	0.264
HRM-2-62	90.183	4.541	0.693	0.039	0.469	0.016
HRM-2-63	306.921	34.109	0.552	0.085	0.243	0.002
HRM-2-64	17.496	0.919	0.741	0.012	2.119	0.404
HRM-2-65	8.356	0.415	0.745	0.009	2.649	1.168

HRM-2-66	27.819	0.649	0.713	0.011	3.432	0.370
HRM-2-67	38.352	1.917	0.659	0.017	2.201	0.171
HRM-2-68	13.828	0.526	0.725	0.011	2.738	0.657
HRM-2-69	32.644	0.960	0.695	0.011	3.232	0.287
HRM-2-70	0.690	0.302	0.917	0.190	0.000	0.003
HRM-2-71	-0.418	0.998	0.271	0.296	0.000	0.001
HRM-2-72	1.214	1.417	0.314	0.457	0.000	0.000
HRM-2-73	0.516	0.213	0.898	0.452	0.000	0.001
HRM-2-74	4.212	0.852	0.993	0.225	0.003	0.003
HRM-2-75	2.894	1.740	0.387	0.622	0.001	0.001
HRM-2-76	13.922	7.461	0.694	0.635	0.005	0.001
HRM-2-77	5.854	2.395	1.026	0.490	0.004	0.002
HRM-2-78	0.462	0.475	0.761	0.435	0.000	0.000
HRM-2-79	8.722	3.661	0.844	0.404	0.003	0.001
HRM-2-80	1.376	1.330	0.236	0.463	0.001	0.001
HRM-2-81	2.868	8.851	0.694	0.653	0.003	0.001
HRM-2-82	8.597	4.056	0.249	0.838	0.004	0.002
HRM-2-83	0.576	0.049	0.805	0.048	0.003	0.019
HRM-2-84	37.320	1.948	0.676	0.040	0.181	0.015
HRM-2-85	20.868	1.135	0.767	0.032	0.186	0.029
HRM-2-86	13.060	1.488	0.757	0.024	0.526	0.229
HRM-2-87	12.316	1.420	0.760	0.021	0.388	0.160
HRM-2-88	56.011	3.239	0.801	0.051	0.208	0.011
HRM-2-89	11.097	1.119	0.853	0.108	0.016	0.005
HRM-2-90	156.630	11.038	0.698	0.068	0.282	0.005
HRM-2-91	18.508	0.605	0.772	0.036	0.180	0.031
HRM-2-92	54.706	4.204	0.725	0.071	0.079	0.005
HRM-2-93	12.691	0.582	0.795	0.059	0.039	0.009
HRM-2-94	41.829	3.675	0.761	0.095	0.049	0.003
HRM-2-95	250.872	26.755	0.822	0.253	0.248	0.002
HRM-2-96	164.370	23.463	0.885	0.283	0.138	0.002
HRM-2-97	48.014	1.962	0.743	0.034	0.356	0.022
HRM-2-98	142.661	10.149	0.851	0.095	0.287	0.007
HRM-2-99	309.063	30.263	0.561	0.081	0.342	0.002
HRM-3						
HRM-3-1	21.883	7.972	1.086	0.643	0.024	0.004
HRM-3-2	62.290	57.204	0.690	0.563	0.056	0.003
HRM-3-3	87.782	14.777	1.026	0.280	0.198	0.010
HRM-3-4	5.275	0.277	0.774	0.052	0.107	0.061
HRM-3-5	44.177	22.208	0.994	0.724	0.046	0.004
HRM-3-6	5.844	0.503	0.885	0.106	0.025	0.018
HRM-3-7	10.237	0.343	0.777	0.038	0.214	0.065
HRM-3-8	40.284	2.440	0.773	0.051	0.286	0.023
HRM-3-9	130.248	25.084	1.132	0.439	0.272	0.013
HRM-3-10	1.750	0.084	0.763	0.019	0.149	0.274

HRM-3-11	4.219	0.237	0.857	0.093	0.106	0.072
HRM-3-12	19.014	7.315	1.125	1.326	0.032	0.015
HRM-3-13	21.856	33.704	0.876	1.791	0.046	0.007
HRM-3-14	80.714	12.458	1.051	0.212	0.188	0.009
HRM-3-15	76.699	43.986	0.674	0.154	0.252	0.042
HRM-3-16	201.708	55.607	0.826	0.268	0.319	0.007
HRM-3-17	1.666	0.043	0.769	0.019	0.106	0.197
HRM-3-18	125.127	54.359	1.109	0.390	0.205	0.011
HRM-3-19	23.838	7.228	1.607	0.765	0.053	0.025
HRM-3-20	99.266	75.185	0.554	0.516	0.310	0.033
HRM-3-21	287.596	89.678	0.908	0.551	0.258	0.002
HRM-3-22	80.535	98.058	0.734	0.854	0.208	0.004
HRM-3-23	4.257	0.104	0.748	0.018	0.315	0.224
HRM-3-24	52.861	14.362	0.768	0.327	0.147	0.012
HRM-3-25	178.388	77.919	1.020	0.673	0.352	0.008
HRM-3-26	202.207	138.769	0.682	0.441	0.366	0.005
HRM-3-27	6.746	0.410	0.782	0.028	0.244	0.124
HRM-3-28	2.859	0.079	0.765	0.020	0.122	0.135
HRM-3-29	134.962	39.014	0.941	0.288	0.161	0.004
HRM-3-30	55.010	6.063	0.708	0.034	0.960	0.075
HRM-3-31	216.838	48.457	0.850	0.246	0.259	0.005
HRM-3-32	208.573	63.752	0.871	0.422	0.333	0.007
HRM-3-33	35.260	9.546	0.876	0.209	0.299	0.032
HRM-3-34	12.114	0.784	0.747	0.022	0.722	0.177
HRM-3-35	47.268	1.421	0.745	0.022	3.001	0.191
HRM-3-36	46.894	1.214	0.732	0.018	4.496	0.276
HRM-3-37	380.849	162.035	0.545	0.171	0.856	0.007
HRM-3-38	203.679	107.683	0.796	0.724	0.351	0.003
HRM-3-39	28.370	1.124	0.741	0.032	0.675	0.065
HRM-3-40	78.731	10.352	0.977	0.231	0.164	0.006
HRM-3-41	82.955	9.459	0.802	0.099	0.321	0.014
HRM-3-42	61.769	1.551	0.717	0.018	4.833	0.222
HRM-3-43	49.153	1.362	0.747	0.023	2.596	0.154
HRM-3-44	194.805	80.151	0.654	0.248	0.158	0.004
HRM-3-45	112.241	54.868	0.625	0.340	0.214	0.004
HRM-3-46	91.760	9.517	0.931	0.138	0.232	0.009
HRM-3-47	32.619	2.905	0.815	0.097	0.103	0.011
HRM-3-48	74.460	33.026	1.001	0.333	0.140	0.005
HRM-3-49	33.871	3.983	0.860	0.128	0.078	0.008
HRM-3-50	18.107	8.577	0.747	0.351	0.017	0.003
HRM-3-51	9.667	1.722	1.034	0.209	0.021	0.010
HRM-3-52	15.028	1.556	0.889	0.123	0.037	0.009
HRM-3-53	27.924	2.182	0.813	0.085	0.113	0.013
HRM-3-54	16.331	3.110	1.014	0.185	0.026	0.008
HRM-3-55	26.222	2.900	0.756	0.103	0.066	0.008

HRM-3-56	25.221	2.413	0.814	0.094	0.081	0.012
HRM-3-57	11.614	0.633	0.795	0.056	0.101	0.027
HRM-3-58	27.662	2.778	0.782	0.065	0.178	0.024
HRM-3-59	104.301	23.880	0.738	0.353	0.154	0.005
HRM-3-60	50.152	5.064	0.834	0.116	0.122	0.008
HRM-3-61	109.517	66.527	0.614	0.362	0.201	0.003
HRM-3-62	96.692	42.771	0.820	0.259	0.157	0.003
HRM-3-63	39.360	3.730	0.813	0.085	0.154	0.012
HRM-3-64	118.742	24.285	0.900	0.245	0.117	0.005
HRM-3-65	254.890	124.491	0.515	0.295	0.219	0.002
HRM-3-66	11.710	0.584	0.876	0.079	0.086	0.025
HRM-3-67	12.265	0.530	0.738	0.042	0.122	0.030
HRM-3-68	59.691	11.028	0.979	0.255	0.130	0.008
HRM-3-69	95.054	98.376	0.276	0.483	0.109	0.001
HRM-3-70	87.266	67.450	0.336	0.317	0.123	0.003
HRM-3-71	21.768	2.583	0.812	0.095	0.060	0.010
HRM-3-72	112.364	35.489	0.847	0.210	0.176	0.005
HRM-3-73	110.084	29.964	0.736	0.301	0.108	0.004
HRM-3-74	11.425	0.508	0.790	0.048	0.150	0.039
HRM-3-75	9.278	0.304	0.771	0.030	0.249	0.088
HRM-3-76	22.693	1.568	0.775	0.062	0.154	0.022
HRM-3-77	63.320	5.480	0.754	0.084	0.251	0.011
HRM-3-78	1.757	0.053	0.761	0.014	0.226	0.399
HRM-3-79	75.197	10.604	0.801	0.142	0.139	0.007
HRM-3-80	4.865	0.194	0.780	0.037	0.091	0.059
HRM-3-81	7.604	0.468	0.795	0.047	0.109	0.048
HRM-3-82	32.497	1.812	0.734	0.049	0.289	0.028
HRM-3-83	7.723	0.246	0.738	0.026	0.290	0.111
HRM-3-84	1.765	0.050	0.765	0.025	0.079	0.139
HRM-3-85	34.372	15.076	0.641	0.345	0.040	0.004
HRM-3-86	8.349	0.482	0.821	0.069	0.054	0.019
HRM-3-87	50.043	3.473	0.666	0.073	0.185	0.010
HRM-3-88	50.985	2.500	0.682	0.056	0.344	0.020
HRM-3-89	6.651	0.738	1.022	0.129	0.017	0.009
HRM-3-90	2.700	0.113	0.758	0.033	0.134	0.152
HRM-3-91	4.064	0.365	0.819	0.042	0.054	0.051
HRM-3-92	1.926	0.056	0.755	0.025	0.093	0.145
HRM-3-93	2.712	0.088	0.736	0.020	0.161	0.181
HRM-3-94	11.236	0.612	0.763	0.058	0.086	0.024
HRM-3-95	23.328	1.531	0.826	0.077	0.135	0.018
HRM-3-96	5.293	0.182	0.762	0.030	0.169	0.094
HRM-3-97	49.178	133.635	0.862	0.358	0.209	0.007
HRM-3-98	55.319	4.182	0.777	0.084	0.225	0.015
HRM-4						
HRM-4-1	472.986	41.904	0.422	0.068	1.328	0.004

HRM-4-2	143.653	10.926	0.689	0.049	1.451	0.028
HRM-4-3	528.150	255.636	0.513	0.194	0.683	0.004
HRM-4-4	521.696	161.447	0.452	0.218	0.651	0.002
HRM-4-5	669.826	168.985	0.479	0.584	0.688	0.004
HRM-4-6	401.682	30.891	0.527	0.066	1.580	0.009
HRM-4-7	25.998	4.951	0.773	0.045	0.493	0.216
HRM-4-8	149.432	11.304	0.725	0.067	1.005	0.020
HRM-4-9	47.099	5.176	0.783	0.029	1.685	0.211
HRM-4-10	80.429	5.927	0.744	0.052	0.862	0.036
HRM-4-11	44.750	8.152	0.770	0.053	0.422	0.072
HRM-4-12	98.622	14.207	0.812	0.098	0.379	0.015
HRM-4-13	401.434	56.957	0.621	0.118	0.879	0.005
HRM-4-14	196.007	21.444	0.693	0.107	0.568	0.007
HRM-4-15	12.278	1.562	0.806	0.042	0.211	0.071
HRM-4-16	23.396	1.338	0.813	0.051	0.270	0.036
HRM-4-17	63.827	7.699	0.781	0.090	0.263	0.018
HRM-4-18	4.704	0.174	0.813	0.024	0.288	0.201
HRM-4-19	2.942	0.098	0.804	0.015	0.710	0.783
HRM-4-20	8.645	1.189	0.816	0.027	0.875	0.661
HRM-4-21	3.069	0.098	0.799	0.015	0.758	0.813
HRM-4-22	1.060	0.033	0.798	0.013	0.341	1.039
HRM-4-23	2.038	0.065	0.810	0.012	0.573	0.914
HRM-4-24	72.127	2.806	0.769	0.037	1.454	0.064
HRM-4-25	827.185	102.666	0.310	0.099	1.833	0.001
HRM-4-26	7.337	0.279	0.794	0.020	1.390	0.614
HRM-4-27	11.288	1.542	0.802	0.040	1.401	0.609
HRM-4-28	1043.655	252.264	0.275	0.167	1.138	0.002
HRM-4-29	716.245	81.429	0.239	0.071	1.530	0.003
HRM-4-30	526.770	75.198	0.405	0.092	1.578	0.009
HRM-4-31	18.954	0.579	0.793	0.024	1.017	0.172
HRM-4-32	38.897	3.593	0.874	0.103	0.183	0.016
HRM-4-33	82.210	8.236	0.783	0.051	0.830	0.035
HRM-4-34	371.300	38.843	0.479	0.061	1.577	0.010
HRM-4-35	83.806	11.204	0.923	0.113	0.262	0.011
HRM-4-36	73.185	9.739	0.753	0.083	0.321	0.016
HRM-4-37	245.795	24.230	0.687	0.101	0.640	0.008
HRM-4-38	484.917	107.262	0.647	0.293	0.496	0.004
HRM-4-39	330.655	103.624	0.479	0.364	0.292	0.003
HRM-4-40	16.051	0.803	0.816	0.025	0.719	0.151
HRM-4-41	32.031	2.458	0.769	0.040	0.451	0.051
HRM-4-42	175.453	44.599	0.726	0.347	0.311	0.007
HRM-4-43	529.940	99.577	0.444	0.228	0.503	0.001
HRM-4-44	442.464	51.080	0.553	0.105	0.978	0.005
HRM-4-45	460.481	120.834	0.381	0.520	0.793	0.003
HRM-4-46	25.449	0.876	0.780	0.034	0.693	0.086

HRM-4-47	34.071	3.855	0.787	0.050	0.478	0.065
HRM-4-48	19.849	2.731	0.845	0.040	0.747	0.319
HRM-4-49	215.508	34.308	0.609	0.155	0.342	0.004
HRM-4-50	525.720	108.203	0.476	0.232	0.797	0.002
HRM-4-51	487.493	68.156	0.517	0.163	1.024	0.005
HRM-4-52	22.529	0.883	0.803	0.031	0.587	0.083
HRM-4-53	24.156	1.250	0.784	0.035	0.473	0.064
HRM-4-54	98.582	10.973	0.805	0.086	0.299	0.010
HRM-4-55	146.780	12.576	0.741	0.081	0.636	0.012
HRM-4-56	394.682	67.021	0.478	0.133	0.856	0.004
HRM-4-57	497.460	63.896	0.539	0.112	1.099	0.004
HRM-4-58	17.374	0.698	0.791	0.026	0.743	0.148
HRM-4-59	22.520	1.022	0.784	0.035	0.477	0.069
HRM-4-60	218.133	81.696	1.157	0.603	0.225	0.003
HRM-4-61	34.747	5.163	0.797	0.037	0.471	0.081
HRM-4-62	414.981	37.579	0.531	0.089	1.046	0.004
HRM-4-63	35.144	2.144	0.759	0.039	0.752	0.072
HRM-4-64	20.327	2.504	0.810	0.042	0.597	0.149
HRM-4-65	65.006	10.788	0.920	0.185	0.147	0.009
HRM-4-66	82.176	5.180	0.781	0.041	0.944	0.037
HRM-4-67	20.765	0.922	0.808	0.029	0.843	0.131
HRM-4-68	38.004	15.034	0.883	0.261	0.072	0.007
HRM-4-69	121.577	16.904	0.721	0.078	0.480	0.016
HRM-4-70	28.648	1.995	0.783	0.024	0.963	0.125
HRM-4-71	19.697	1.171	0.788	0.025	0.863	0.150
HRM-4-72	17.058	1.115	0.793	0.027	0.891	0.187
HRM-4-73	2.122	0.035	0.802	0.012	0.521	0.775
HRM-4-74	491.937	122.321	0.613	0.220	0.897	0.004
HRM-4-75	362.599	81.459	0.604	0.083	1.212	0.009
HRM-4-76	663.086	124.576	0.407	0.232	0.933	0.002
HRM-4-77	741.417	177.771	0.323	0.218	1.315	0.002
HRM-4-78	496.012	64.040	0.517	0.096	1.462	0.006
HRM-4-79	952.654	140.223	0.118	0.183	1.044	0.000
HRM-4-80	230.034	298.407	0.861	0.853	0.767	0.004
HRM-4-81	656.970	76.399	0.417	0.105	1.511	0.003
HRM-4-82	488.705	48.011	0.373	0.075	1.211	0.003
HRM-4-83	378.808	323.415	0.526	0.463	0.939	0.004
HRM-4-84	322.645	77.445	0.867	0.265	0.570	0.005
HRM-4-85	451.828	128.866	0.466	0.312	0.739	0.002
HRM-4-86	413.756	71.722	0.758	0.200	0.649	0.005
HRM-4-87	168.234	61.195	0.646	0.345	0.607	0.012
HRM-4-88	241.805	37.211	0.841	0.174	0.655	0.008
HRM-4-89	377.122	73.811	0.942	0.437	0.799	0.004
HRM-4-90	401.850	156.712	0.461	0.375	0.707	0.001
HRM-4-91	427.906	107.500	0.564	0.305	0.728	0.003

HRM-4-92	356.624	122.076	1.076	0.465	0.492	0.002
HRM-4-93	300.731	35.669	0.677	0.122	0.690	0.005
HRM-4-94	273.918	136.541	0.476	0.847	0.732	0.005
HRM-4-95	337.872	139.017	0.401	0.724	0.494	0.002
HRM-4-96	304.534	91.787	0.843	0.400	0.783	0.007
HRM-4-97	620.145	148.874	0.479	0.244	0.910	0.002
HRM-4-98	272.071	28.181	0.574	0.101	0.580	0.005
HRM-4-99	295.223	29.362	0.780	0.119	1.089	0.010
HRM-4-100	236.566	17.220	0.616	0.070	1.023	0.010

Supplementary References

Aksoy, E., İnceöz, M., Koçyiğit, A. Lake Hazar Basin: A Negative Flower Structure on the East Anatolian Fault System (EAFS), SE Turkey, Turkish Journal of Earth Sciences (Turkish J. Earth Sci.), Vol. 16, pp. 319-338 (2007).

Aktuğ, B., Özener, H., Doğru, A., Sabuncu, A., Turgut, B., Halıcıoğlu, K., Havazlı, E. Slip rates and seismic potential on the East Anatolian Fault System using an improved GPS velocity field. J. Geodyn. **94**, 1–12 (2016).

Allen, M.B., Jackson, J., Walker, R. Late Cenozoic reorganization of the Arabia–Eurasia collision and the comparison of short-term and long-term deformation rates. Tectonics, **23**, TC2008 https://doi.org/10.1029/2003TC001530 (2004).

Altunel, E., Meghraoui, M., Karabacak, V., Akyüz, S., Ferry, M., Yalçıner, Ç., Munschy, M. Archaeological sites (Tell and Road) offset by the Dead Sea Fault in the Amik Basin, Southern Turkey, Geophys. J. Int., **179**, 1313-1329 (2009).

Arpat, E., Şaroğlu, F. Doğu Anadolu Fayı ile İlgili Bazı Gözlemler ve Düşünceler. Bulletin of the Mineral Research and Exploration, **78**(78), 44-50 (1972).

Arpat, E., Şaroğlu, F. Türkiye'deki bazı önemli genç tektonik olaylar, TJK Bülteni, **18**, 91-101 (1975).

Bakkal, B., Cengiz Cinku, M. & Heller, F. Paleomagnetic results along the Bitlis-Zagros suture zone in SE Anatolia, Turkey: Implications for the activation of the Dead Sea Fault Zone. Journal of Asian Earth Sciences **172**, 14–29 https://doi.org/10.1016/j.jseaes.2018.08.026 (2019).

Barka, A., and Reilinger, R. Active tectonics of the Mediterranean region: Deduced from GPS, neotectonic and seismicity data, Annali di Geofisica, XI, 3, 587-609 (1997).

Bertrand, S. Tectonique active a la jonction des plaques Africa, Arabie et Anatolie-Eurasie (sud de la Turquie): caracterisation des failles et analyse de la deformation par un reseau GPS dense, Doktora Tezi, Institut de Physique du Globe de Strasbourg, (yayınlanmamış) (2006).

Boles, A., van der Pluijm, B., Mulch, A., Mutlu, H., Uysal, I.T., and Warr, L.N. Hydrogen and 40Ar/ 39Ar isotope evidence for multiple and protracted paleofluid flow events within the long-lived North Anatolian Keirogen (Turkey), Geochem. Geophys. Geosyst.,**16**, 1975–1987 https://doi.org/10.1002/2015GC005810 (2015).

Brun, J.-P., Faccenna, C., Gueydan, F., Sokoutis, D., Philippon, M., Kydonakis, K., Gorini, C. The two-stage Aegean extension, from localized to distributed, a result of slab rollback acceleration. Can. J. Earth Sci. **53**, 1142–1157 https://doi.org/10.1139/cjes-2015-0203 (2016).

Çetin, H., Güneyli, H., Mayer, L. Paleosismology of the Palu-Lake Hazar segment of the East Anatolian Fault Zone, Turkey, Tectonophysics, **374**, 163-197 (2003).

Çetiner, U., van Hunen, J., Göğüş, O.H., Valentine, A.P., Allen, M.B. How double-slab subduction shaped the Eastern Anatolian Plateau: Insights from geodynamic models. Geology, **53**(10), 837-841 (2025).

Dewey, J.F., Hempton, M.R., Kidd, W.S.F., Saroglu, F., Şengör, A.M.C. Shortening of continental lithosphere: The neotectonics of Eastern Anatolia-A young collision zone. Geological Society, London, Special Publications, **19**, 1-36 (1986).

Faccenna, C., Bellier, O., Martinod, J., Piromallo, C., Regard, V. Slab detachment beneath eastern Anatolia: A possible cause for theformation of the North Anatolian fault, Earth Planet. Sci. Lett., **242**(1), 85–97 (2006).

Garfunkel, Z. and Ben-Avraham, Z. The Structure of the Dead Sea basin. Tectonophysics, **266**, 155-176 (1996).

Garfunkel, Z. Internal Structure of the Dead Sea leaky transform (rift) in relation plate kinematics. Tectonophysics, **80**, 81-108 (1981).

Güneyli, H. Doğu Anadolu Fay Sistemi, Palu-Hazar Gölü Segmentinin Neotektoniği ve Paleosismolojisi, Ç.Ü. F.B.E., Doktora Tezi, 143 (2002).

Hempton, M. R. Structure and deformation history of the Bitlis suture near Lake Hazar, southeastern Turkey, Geol. Soc. Am. Bull., **96**, 233-243 (1985).

Hempton, M.R. Constrains on Arabian Plate Motion and Extensional History of the Red Sea. Tectonics, **6**(6), 687-705 doi:10.1029/TC006i006p00687 (1987).

Herece, E. Doğu Anadolu Fayı, 56. Türkiye Jeoloji Kurultayı Bildiri Özleri, MTA, Ankara, s. 309-310 (2003).

Herece, E., and Akay, E. Karlıova-Çelikhan arasında Doğu Anadolu Fayı, Türkiye 9. Petrol Kongresi, 361-372 (1992).

Hubert-Ferrari, A., Lamair, L., Hage, S., Schmidt, S., Çağatay, M.N., Avşar, U. A 3800 yr paleoseismic record (Lake Hazar sediments, eastern Turkey): Implications for the East Anatolian Fault seismic cycle. Earth and Planetary Science Letters, **538**, 116152 https://doi.org/10.1016/j.epsl.2020.116152 (2020).

Karabacak, V. Quaternary Activity of the Northern Dead Sea Fault Zone. PhD thesis, Eskisehir Osmangazi University, Natural and Applied Sciences Institute [in Turkish with English abstract]. (2007).

Karabacak, V., Altunel, E., Meghraoui, M., Akyüz, H. S. Field evidences from northern Dead Sea Fault Zone (South Turkey): New findings for the initiation age and slip rate, Tectonophysics, **480**, 172–182 https://doi.org/10.1016/j.tecto.2009.10.001 (2010).

Karabacak, V., Yönlü, Ö., Altunel, E., Kıyak, N.G., Akyüz, H.S., Yalçıner, C.Ç. Paleoseismic behavior of the east anatolian fault zone between Gölbaşı and Türkoğlu: implications on 900 years of seismic quiescence. In: International Earth Science Colloquium on the Aegean Region. IESCA-2012, p 110 (2012).

Kasapoğlu, K.E. Doğu Akdeniz'in sismotektonik özellikleri: sonlu elemanlar çözümlemesi (Seismotectonic charecteristics of eastern Mediterranean: a finite element analysis), Yerbilimleri **14**, 309– 317 (1987).

Keskin, M. Magma generation by slab steepening and breakoff beneath a subduction-accretion complex: An alternative model for collision-related volcanism in Eastern Anatolia, Turkey. Geophysical Research Letters, **30**(24), 8046 (2003).

Kiratzi, A.A study on the active crustal deformation of the North and East Anatolian Fault Zones, Tectonophysics, **225**, 191-203 (1993).

Koçyiğit, A., Yılmaz, A., Adamia, S., Kuloshvili, S. Neotectonics of East Anatolian Plateau (Turkey) and Lesser Caucasus: implication for transition from thrusting to strike-slip faulting. Geodinamica Acta **14**, 177–195 (2001).

Le Pichon, X., Kreemer, C. The Miocene-to-Present kinematic evolution of the Eastern Mediterranean and Middle East and its implications for dynamics. *Annual Review of Earth and Planetary Sciences* **38**, 323–351 (2010).

Lin, Y.C., Chung, S.L., Bingöl, A.F., Yang, L., Okrostsvaridze, A., Pang, K.N., Lee, H.Y., Lin, T.H. Diachronous initiation of post-collisional magmatism in the Arabia-Eurasia collision zone. Lithos, 356-357, 105394 (2020).

Lyberis, N., Tekin, Y., Chorowicz, J., Kasapoğlu, E., Gündoğdu, N. The East Anatolian Fault: an oblique collisional belt, Tectonophysics, **204**, 1-15 (1992).

Mahmoud, Y., Masson, F., Meghraoui, M., Cakir, Z., Alchalbi, A., Yavasoglu, H., Yönlü, Ö., Daoud, M., Ergintav, S., Inan, S. Kinematic study at the junction of the East Anatolian fault and the Dead Sea fault from GPS measurements. J. Geodyn. **67**, 30–39 https://doi.org/10.1016/j.jog.2012.05.006 (2013).

McClusky, S., Balassanian, S., Barka, A., Demir, C., Ergintav, S., Georgiev, I., Gürkan, O., Hamburger, M., Hurst, K., Kahle, H., Kastens, K., Kekelidze, G., King, R., Kotzev, V., Lenk, O., Mahmoud, S., Mishin, A., Nadriya, M., Ouzounins, A., Paradissis, D., Peter, Y., Prilepin, M., Reilinger, R., Sanli, I, Seeger, H., Tealeb, A., Toksöz, M. N., Veis, G. Global Positioning System constraints on plate kinematics and dynamics in the eastern Mediterranean and Caucasus, J.Geophy.Res., **105**, 5695-5720 (2000).

Mutlu, H., Uysal, I.T., Altunel, E., Karabacak, V., Feng, Y., Zhao, J.-X., and Atalay, O. Rb- Sr systematics of fault gouges from the North Anatolian fault zone (Turkey): Journal of Structural Geology, v. **32**, p. 216–221 https://doi.org/10.1016/j.jsg.2009.11.006 (2010).

Nuriel, P. et al. The onset of the Dead Sea transform based on calcite age-strain analyses. Geology **45**, 587–590 https://doi.org/10.1130/G38903.1 (2017).

Nuriel, P. et al. Reactivation history of the North Anatolian fault zone based on calcite age-strain analyses: Geology, v. **47**, p. 1–5 https://doi.org/10.1130/G45727.1 (2019).

Okay, A.I., Zattin, M., Cavazza, W. Apatite fission-track data for the Miocene Arabia-Eurasia collision. Geology, **38** (1): 35–38 doi: https://doi.org/10.1130/G30234.1 (2010).

Oral, M. B., Reilinger, R., Toksöz, R. Deformation of the Anatolian block as deduced from GPS measurements, Transactions, American Geophysical Union, EOS, **73**, 120 (1992).

Quennell, A.M. The Structural and Geomorphic Evolution of the Dead Sea Rift. Quarterly. *Journal of the Geological Society* **114**, 1-24 https://doi.org/10.1144/gsjgs.114.1.0001 (1958).

Reilinger, R., McClusky, S. C., Oral, M. B., King, W. Toksöz, M. N. Global positioning, system measurements of present-day crustal movements in the Arabia-Africa-Eurasia plate collision zone, J.Geophy. Res., **102**, 9983-9999 (1997).

Reilinger, R., McClusky, S., Vernant, P., Lawrence, S., Ergintav, S., Cakmak, R., Ozener, H., Kadirov, F., Guliev, I., Stepanyan, R., Nadariya, M., Hahubia, G., Mahmoud, S., Sakr, K., ArRajehi, A., Paradissis, D., Al-Aydrus, A., Prilepin, M., Guseva, T., Evren, E., Dmitrotsa, A., Filikov, S. V., Gomez, F., Al-Ghazzi, R., Karam, G. GPS constraints on continental deformation in the Africa-Arabia-Eurasia continental collision zone and implications for the dynamics of plate interactions, Journal of Geophysical Research-Solid Earth, **111** (B5): Art. B05411, 52 p. https://doi.org/10.1029/2005JB004051 (2006).

Ring, U., J. Glodny, T. Will, and S. Thomson. "The Hellenic Subduction System: High-Pressure Metamorphism, Exhumation, Normal Faulting, and Large-Scale Extension." Annual Review of Earth and Planetary Sciences **38**: 45–76 https://doi.org/10.1146/annurev.earth.050708.170910 (2010).

Rojay B., Heimann, A., Toprak, V. Neotectonic and volcanic characteristics of the Karasu fault zone (Anatolia, Turkey): The transition zone between the Dead Sea transform and the East Anatolian fault zone, Geodinamica Acta, **14**, 197–212 https://doi.org/10.1080/09853111.2001.11432444 (2001).

Şaroğlu, F., Emre, Ö., Boray, A. Türkiye'nin Diri Fayları ve Depremsellikleri. MTA, Ankara (1987).

Seyitoğlu, G., Scott, B.C., Rundle, C.C. Timing of Cenozoic extensional tectonics in west Turkey. Journal of the Geological Society, **149** (4): 533–538 doi: https://doi.org/10.1144/gsjgs.149.4.0533 (1992).

Seymen, İ., Aydın, A. Bingöl deprem fayı ve bunun Kuzey Anadolu Fayı ile ilişkisi, MTA Bülteni, **79**, 1-8 (1972).

Steinz, G., Bartov, Y. The Miocene–Piocene history of the Dead Sea segment of the Rift in the light of K–Ar ages of basalts. Israel Journal of Earth Sciences **40**,199–208 (1991).

Taymaz, T., Eyidoğan, H., Jackson, J. Source parameters of large earthquakes in the EAF (Turkey), Geophy. J. Int., **106**, 537-550 https://doi.org/10.1111/j.1365-246X.1991.tb06328.x (1991).

Uysal, I.T., Karabacak, V., Aykut, T., Ring, U., Liu, E., Sancar, T., Leonard, N., Tong, K., Todd, A.J. and Temel, A. Was the Formation of the North Anatolian Fault Influenced by the Aegean Extension? Terra Nova, **37**: 342-352 https://doi.org/10.1111/ter.12782 (2025).

Uysal, I.T., Mutlu, H., Altunel, E., Karabacak, V., Golding, S.D. Clay mineralogical and isotopic (K–Ar, δ18O, δD) constraints on the evolution of the North Anatolian Fault Zone, Turkey. Earth and Planeatry Science Letters, **243**, 181-194 https://doi.org/10.1016/j.epsl.2005.12.025 (2006).

van Hinsbergen, D.J., Gürer, D., Koç, A., Lom, N., Shortening and extrusion in the East Anatolian Plateau: How was Neogene Arabia-Eurasia convergence tectonically accommodated? *Earth Planet. Sci. Lett*. **641**, 118827 (2024).

Westaway, R. Kinematic consistency between the Dead Sea Fault Zone and the Neogene and Quaternary left-lateral faulting in SE Turkey, Tectonophysics, **391**, 203-237 (2004).

Westaway, R. Kinematics of the Middle East and Eastern Mediterranean Updated, Turkish J.Earth Sci. J., **12**, 5-46 (2003).

Westaway, R., Arger, J. The Gölbaşı basin, southeastern Turkey: A complex discontinuity in a major strike-slip fault zone, J. Geol. Soc., London, **153**, 729-743 (1996).

Yönlü, Ö. and Karabacak, V., "Surface rupture history and 18 kyr long slip rate along the Pazarcık segment of the East Anatolian Fault," GEOLOGICAL SOCIETY. JOURNAL, vol.**181**, no.1, pp.1-11 https://doi.org/10.1144/jgs2023-056 (2024).

Yurtmen, S., Rowbotham, G., İşler, F., Floyd, P. A., Petrogenesis of basalts from Southern Turkey: The Plio-Quaternary volcanism to the North of İskenderun Gulf. Tectonics and Magmatism in Turkey and the Surrounding Area, Geological Society, London, special Publications, **173**, 489-512 https://doi.org/10.1144/gsl.sp.2000.173.01.23 (2000).

Yürür, M. T., Chorowicz, J. Recent volcanism, tectonics and plate kinematics near the junction of the African, Arabian and Anatolian plates in the Eastern Mediterranean, Journal of Volcanology and Geothermal Research, **85**, 1-15 (1998).